

VIX vs VXX: A Joint Analytical Framework

Martino Grasselli* Lakshithe Wagalath†

March 20, 2018

Abstract

We propose a framework for modeling in a consistent manner the VIX index and the VXX, an exchange-traded note written on the VIX. Our study enables to link the properties of VXX to those of the VIX in a tractable way. In particular, we quantify the systematic loss observed empirically for VXX when the VIX futures term-structure is in contango and we derive option prices, implied volatilities and skews of VXX from those of VIX in infinitesimal developments. We also perform a calibration on real data which highlights the flexibility of our model in fitting the futures and the vanilla options market of VIX and VXX. Our framework can be used to model other exchange-traded notes on the VIX as well as any market where exchange-traded notes have been introduced on a reference index, hence providing tools to better anticipate and quantify systematic behavior of an exchange-traded note with respect to the underlying index.

Keywords: volatility index, VIX, VIX exchange-traded notes, VXX.

JEL classification: G11, G15, G21.

1 Introduction

Over the last decades financial markets have witnessed a significant and steady increase in the number of volatility-related products. Since the subprime crisis, the demand for volatility instruments accelerated, in a context of pronounced market uncertainty (Sussman and Morgan, 2012). Among all volatility instruments, the VIX index, created by the CBOE in 1993, is considered as a landmark by most market players. As calculated originally, the VIX captured the 30-day at-the-money implied volatility of options in the S&P 500 index. Its calculation has been slightly revised in 2004 in order to take into account also the skew of options on the S&P 500 (CBOE, 2014).

The VIX quickly became a “fear gauge” for investors, providing a measure for the nervousness of equity markets. It became tradable via futures in 2004 and options in 2006, hence providing market players new instruments to trade implied volatility in a direct manner (Whaley, 2008). Since then, volumes on VIX futures and options skyrocketed. For example, in 2015, the VIX became the second most traded underlying in the CBOE options market (CBOE, 2016), right after the S&P 500 itself.

Yet, as currently designed by the CBOE, derivatives on the VIX may be inaccessible to non-institutional players, mainly due to the large notional sizes of the contracts. This motivated the introduction of exchange-traded notes (ETNs) on the VIX. In 2009, Barclays launched the first two ETNs on the VIX: VXX and VXZ. Typically, Barclays delivers to VXX holders a daily return equal to a combination of the daily return of two futures on the VIX, so as to track a synthetic 30-day VIX futures. Since then, ETNs on the VIX flourished: there currently exist more than thirty of them, with several billion dollars in market caps and daily volumes (see Alexander and Korovilas (2013) for a comprehensive empirical study on VIX ETNs).

While the introduction of ETNs on VIX enabled new investors to trade market volatility while enjoying the benefits of small nominals and bid-ask spreads, the performance of those products raised

*Department of Mathematics, University of Padova (Italy) and Devinci Research Center, Léonard de Vinci Pôle Universitaire, 92 916 Paris La Défense (France). Email: grassell@math.unipd.it.

†IESEG School of Management (LEM CNRS). Email: l.wagalath@ieseg.fr

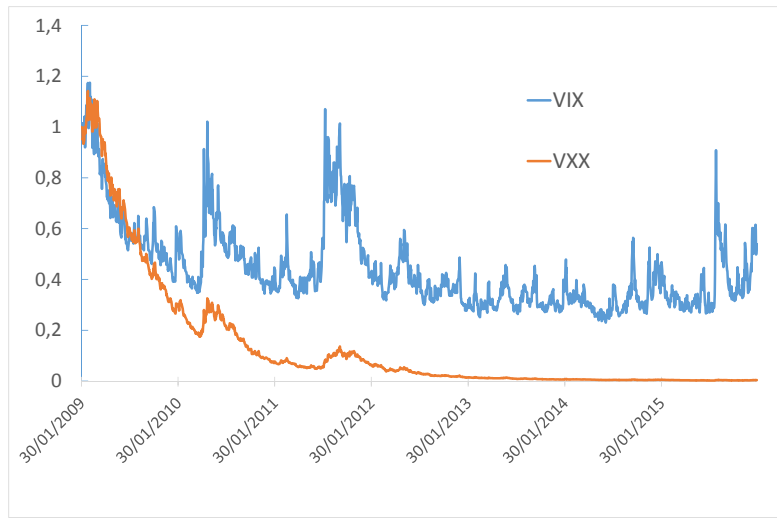


Figure 1: Prices of VIX and VXX

concerns among market players and regulators (Bloomberg, 2012). Figure 1 shows the remarkable underperformance of VXX compared to VIX. Whereas many market players use VXX as a proxy for trading VIX in a cheap manner, in the VXX prospectus (see (Barclays, 2016)) Barclays warns VXX holders that “Your ETN is not Linked to the VIX index and the value of your ETN may be less than it would have been had your ETN been linked to the VIX Index”. This discrepancy between VIX and VXX is confirmed by Figure 2, which shows the linear regression of daily returns of VIX on VXX and the one-year realized correlation between the two securities.

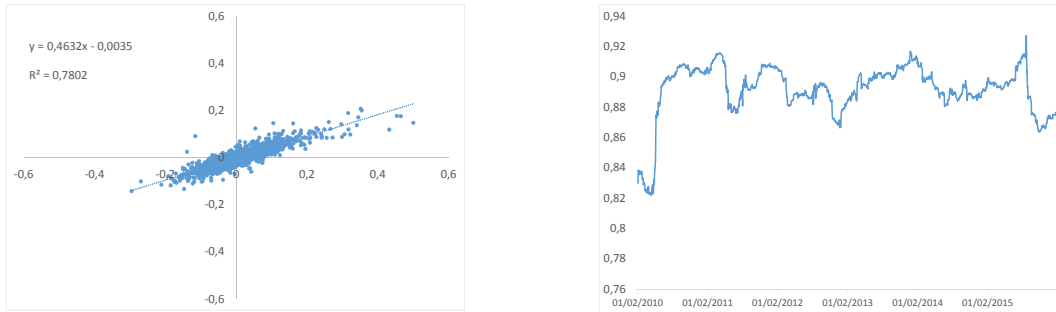


Figure 2: Left: Linear regression of VIX vs VXX daily returns; Right: One-year realized correlation between VIX and VXX daily returns

While this feature may be explained in an intuitive manner from the way VXX is calculated (see Subsection 3.2 for an explicit formula for VXX daily return calculation), the popularity of VXX and other VIX ETNs calls for a quantitative framework for modeling VIX and its related ETNs in a consistent manner. This would enable to link the characteristics of the VIX and its derivatives – daily return, implied volatility, skew – to that of its ETNs in a tractable way and hence better model VIX ETNs, and anticipate their unexpected or undesired behavior.

In this paper, we develop a methodology to model the VIX and VXX in a consistent manner. The main contribution of our work is to propose a model that is rich enough so as to reproduce the joint properties of the VIX and the VXX – term structure of futures, implied volatility – and flexible enough so as to link the drift, volatility and skew of the VXX to that of the VIX in a tractable manner. We also show that it is possible to lead a joint calibration of VIX futures, options and VXX options. To our knowledge, we are the first study that proposes such joint calibration exercise using the real formula the real VXX formula, and not an approximate one, as usually done in the literature. The framework that we develop is very generic and can be used to model any other ETN on the VIX or, more generally, any ETN built on a reference index.

Related literature: Theoretical studies on the VIX can be divided into two strands of literature: on the one hand, the consistent-pricing approach models the joint (risk-neutral) dynamics of the S&P 500 and the VIX with, most often, the aim of pricing derivatives on the two indices in a consistent manner (see Cont and Kokholm (2013) for a review of the existing literature); on the other hand the stand-alone approach directly models the dynamics of the VIX. The first stand-alone model for the VIX was proposed by Whaley himself, who had been hired by the CBOE to develop the methodology for computing the VIX: Whaley (1993) models the spot VIX as a geometric Brownian motion,

$$\frac{dVIX_t}{VIX_t} = rdt + \sigma dW_t,$$

hence enabling to price options on the VIX in the Black and Scholes framework, but failing to capture the smile effect and the mean-reversion of volatility processes, which is necessary in order to fit the term structure of futures prices (Schwert, 1990; Pagan and Schwert, 1990; Schwert, 2011). Since then, numerous stand-alone models have been proposed for the VIX. We refer to Bao et al. (2012); Lin (2013) for a detailed review on that strand of literature. Let us cite the two seminal models proposed on the topic. Grünbichler and Longstaff (1996) model the spot VIX as a square root process, similar to the dynamics of the instantaneous variance in the (Heston, 1993) model:

$$dVIX_t = \alpha(\beta - VIX_t)dt + \Lambda\sqrt{VIX_t}dW_t.$$

The presence of a mean reversion in the drift allows the possibility to reproduce different shapes for the term structure of futures prices, which take the form

$$F_{VIX}^{SQR}(t, T) = \mathbb{E}^Q [VIX_T | \mathcal{F}_t] = \beta + (VIX_t - \beta)e^{-\alpha(T-t)}.$$

In addition, options prices for vanillas are simple as the distribution of the VIX process is known: however, the model is quite rigid as only negative skews can be reproduced, in contrast with VIX market data. Detemple and Osakwe (2000) model the logarithm of the spot VIX as an Ornstein-Uhlenbeck process:

$$d\log VIX_t = \alpha(\beta - \log VIX_t)dt + \Lambda dW_t,$$

that leads to closed form expressions for futures and vanillas but no skew is permitted as the VIX is lognormal. In those two models and in most stand-alone models for the VIX, the dynamics of the volatility index is driven by one Brownian motion only, which implies some rigidity when it comes to reproducing simultaneously term-structure, implied volatility and skew. A first attempt to tackle this issue is provided by Psychoyios et al. (2009) who extended the model of Detemple and Osakwe (2000) by adding Merton-type jumps in the dynamics of VIX, and then leading to a model that is able to fit also positive skews. Mencia and Sentana (2013) propose an extension of those models by introducing a long-run value for the VIX which is no more a constant but a CIR process itself, driven by a Brownian motion independent from the one appearing in the spot VIX dynamics. In the square root specification for the VIX this reads as

$$\begin{aligned} dVIX_t &= \alpha(\beta_t - VIX_t)dt + \Lambda\sqrt{VIX_t}dW_t^{VIX} \\ d\beta_t &= \bar{\alpha}(\bar{\beta} - \beta_t)dt + \bar{\Lambda}\sqrt{\beta_t}dW_t^\beta, \end{aligned}$$

while in the logarithmic model of Detemple and Osakwe (2000) it becomes

$$\begin{aligned} d \log VIX_t &= \alpha(\beta_t - \log VIX_t)dt + \Lambda dW_t^{VIX} \\ d\beta_t &= \bar{\alpha}(\bar{\beta} - \beta_t)dt + \bar{\Lambda}\sqrt{\beta_t}dW_t^\beta. \end{aligned}$$

Square root and logarithmic specifications for the VIX can be extended to the case where the volatility of the VIX is also stochastic (Kaeck and Alexander, 2013). From the calibration viewpoint, the fit in the square root models is quite scarce, due to the rigidity of the model in managing changes in the skew. On the other hand, it is now clear that there is almost no added value in considering both jumps and stochastic volatility in the model, see e.g. Kaeck and Alexander (2010). What is more, a multi factor specification of the previous models is difficult to handle.

The model that we develop here is similar yet more general in the sense that we allow not only for a stochastic volatility but also for a stochastic drift for the spot VIX and that the two Brownian motions involved in the dynamics of the VIX may be correlated. The idea of introducing a stochastic drift for the VIX, which can be interpreted as a stochastic convenience yield, is motivated by the need to develop a model that is rich enough to reproduce the diverse configurations of VIX futures term-structures, which is necessary to model the VXX in a consistent manner. This idea is similar to Gibson and Schwartz (1990) who model the varying term-structure of futures written on commodities. In their model, the spot price of the commodity and the instantaneous convenience yield are assumed to follow the joint stochastic process

$$\begin{aligned} dS_t &= (\mu - \delta_t)S_t dt + \sigma_S S_t dW_t^S \\ d\delta_t &= \kappa(\alpha - \delta_t)dt + \sigma_\epsilon dW_t^\epsilon, \end{aligned}$$

with correlated Brownian motions W^S and W^ϵ . This (affine) framework allows for closed form expressions for the price of futures and Black-Scholes like formulae for the price of vanilla options. On the other hand, the lognormal distribution of the commodity price prevents the possibility to reproduce the typical smile and skew effects observed in the option market. This drawback can be easily removed by considering a more sophisticated dynamics for the convenience yield, as we are going to show in our application to the VIX/VXX markets. The literature on VXX is scarce. To our knowledge, there are only a few theoretical studies which propose a unified framework for VIX and VXX. Existing studies on the VXX (Bao et al., 2012) rather model the VXX in a stand-alone manner, which obliterates completely the link between VIX and VXX – typically the loss for VXX when the VIX is in contango cannot be anticipated in such models. One remarkable exception is the lognormal 2-factor model proposed by Bergomi, see e.g. Chapter 7 of Bergomi (2016). Bergomi assumes that the VIX can be written as

$$VIX_t = \exp(X_{1t} + X_{2t}),$$

where X_{1t}, X_{2t} are modelled as correlated Ornstein-Uhlenbeck factors. This parsimonious 2-factor model is able to reproduce the stylized facts of the VIX market, including the mean reversion of the VIX, smile and skew of vanillas and it is analytically tractable insofar it leads to closed form expressions for most relevant quantities. Bergomi shows that within this framework the option market on VXX is not redundant. In fact, once the model is calibrated on the VIX market, there is still a degree of freedom in fitting different levels for the implied volatility of the VXX. In other words, VIX smiles do not provide enough information for deducing the implied volatility of the VXX, which is very dependent on assumptions about the distribution of each VIX futures. However, we emphasize that Bergomi (2016) did not perform a joint calibration of the VIX/VXX market as we are going to do in our paper. As far as empirical studies are concerned, we recall the comprehensive work on ETNs on the VIX conducted by Alexander and Korovilas (2013). Their work details the statistical properties of such volatility instruments and explores diverse trading strategies based – among other factors – on rolling costs, that we quantify in our paper. Finally, Avellaneda and Papanicolaou (2017) study the statistical properties of the dynamics of VIX futures and several ETNs/ETFs in a trading perspective. Although

their investigation does not include the option market, they are anyway able to provide a support for the statistical profitability of selling the VIX through its ETNs. In our framework for modeling the joint dynamics for VIX and VXX, we can give a theoretical support for effects like the loss in contango, still being consistent with the option market.

2 Modeling the VIX and pricing its derivatives

We model the risk-neutral dynamics of the VIX index, denoted S throughout the paper, using the following one-factor specification:

$$\frac{dS_t}{S_t} = (r - \delta X_t)dt + \sigma \sqrt{\alpha X_t + \beta} dZ_t, \quad S_0 > 0, \quad (1)$$

where Z is a Brownian motion under the risk-neutral probability \mathbb{Q} and X is a stochastic factor following the stochastic differential equation

$$dX_t = \kappa(\theta - X_t)dt + \omega \sqrt{\alpha X_t + \beta} dW_t, \quad X_0 = x, \quad (2)$$

with W a \mathbb{Q} Brownian motion such that $\text{corr}(W, Z) = \rho$. The coefficient ω may be seen somehow redundant, however it will be useful when studying our developments in the sequel.

As such, the VIX follows a stochastic differential equation with stochastic volatility and stochastic risk-neutral drift. While stochastic volatility has already been used in the literature for pricing VIX options (see section 1), the novelty of our approach is to specify also a stochastic risk-neutral drift. In our framework, the risk-neutral drift of the VIX is driven by the exogenous factor X and will be useful for reproducing VIX futures prices and the various possible configurations of the term structure of VIX futures prices (contango, backwardation, humped and others). As the value of the VXX is directly calculated from the VIX futures prices, it is crucial to use a model which enables to reproduce the complexity of the VIX futures market. To our knowledge, and contrary to most other models that yield rigid structures of VIX futures prices, the one-factor model that we develop here is the first – apart from the 2-factor model developed by Bergomi (2016) – to achieve this goal in the context of VIX and VXX. The stochastic drift of the VIX can be interpreted as a *convenience yield* term, which is commonly used to reproduce the variability of the term structure of futures on commodities. In fact, although the VIX does not pay any dividend, the stochastic drift is mathematically equivalent to a stochastic dividend yield, see e.g. Detemple and Osakwe (2000), Mencia and Sentana (2013), Carmona and Ludkovski (2004), Gibson and Schwartz (1990).

The dynamics of the VIX given in equations 2 and 1 encompasses the benchmark models which have been proposed for the VIX over the last years: geometric Brownian motion (Whaley, 1993) ($\alpha = \delta = 0$), Heston model ($\beta = \delta = 0$), log-normal Ornstein-Uhlenbeck model (Detemple and Osakwe, 2000) ($W = Z$ and $X = \ln(S)$) or the model developed in (Gibson and Schwartz, 1990) for commodities ($\alpha = 0$), who inspired our approach.

Note that we consider a one-dimensional factor for clarity purpose only. However, our study can be easily extended to a multi-factor specification (see appendix) or to a more general Wishart setting (Gourieroux, 2006; Grasselli and Tebaldi, 2008), thus representing the stochastic volatility affine counterpart of the seminal two-factor lognormal model developed by Bergomi (2016).

As we will see in the next section, the value of the VXX is derived from futures prices on the VIX index, and the focus of the paper is to model VIX and VXX and price their derivatives in a consistent manner. As a consequence, in terms of modelling, we naturally choose to model directly the dynamics of the VIX under the risk-neutral probability. We could have started our study by specifying the dynamics of the VIX under the historical probability: in that case, we would need to apply a change of probability measure to obtain the risk-neutral dynamics of the VIX and lead our study. We could also have started our study by specifying the dynamics of the S&P500 itself: we would then need to deduce the risk-neutral dynamics of the VIX in order to study the VXX in a consistent manner.

While the dynamics of the VIX given in equations (1) and (2) is sophisticated enough to reproduce the features of the futures and options written on the VIX, it is also flexible in the sense that it enables to

calculate the price of VIX derivatives in closed-form. The first relevant quantity that we calculate is the futures price at date t for a futures contract written on the VIX with maturity T , which is defined by

$$F(t, T) = \mathbb{E}_t(S_T), \quad (3)$$

where \mathbb{E}_t denote the risk-neutral expectation conditional on date t . The following proposition characterizes the futures price in a tractable manner.

Proposition 2.1. *The futures price at date t for a contract written on the VIX with maturity T is given by*

$$F(t, T) = S_t e^{\Phi(t, T) + X_t \Psi(t, T)} \quad (4)$$

where Φ and Ψ are deterministic functions given explicitly in Appendix 9.2.

The proof of this proposition is given in Appendix 9.2. Applying Ito's formula to equation (4) and using the fact that the futures price is a \mathbb{Q} -martingale, we can deduce that the dynamics of the futures price $F(t, T)$ is given by the stochastic differential equation

$$\frac{dF(t, T)}{F(t, T)} = \sigma \sqrt{\alpha X_t + \beta} dZ_t + \omega \Psi(t, T) \sqrt{\alpha X_t + \beta} dW_t. \quad (5)$$

As one would expect, the volatility of the futures price is a combination of the volatility of the VIX and that of the factor X itself. In particular, when the stochastic factor driving the dynamics of the VIX becomes deterministic ($\omega = 0$), the VIX and its futures contract have the same volatility. Similarly, as we approach maturity and the futures price converges to the spot price, the volatility of the futures contract will be close to that of the VIX. Mathematically, this is due to the fact that, given equation (4), $\Psi(t, T) \rightarrow 0$ when $t \rightarrow T$.

In addition, we can also calculate the price of options written on the VIX. The following proposition gives the price of a VIX Call option in a tractable manner.

Proposition 2.2. *The price, at date 0, of a Call option written on the VIX, with maturity T and strike K is equal to*

$$Call_{VIX}(0) = -\frac{e^{-rT} K}{\pi} \int_0^{+\infty} Re \left[\frac{K^{i\epsilon}}{\epsilon^2 - i\epsilon} \mathbb{E}[e^{-i\epsilon \ln(S_T)}] \right] d\epsilon. \quad (6)$$

The proof of this proposition is given in Appendix 9.3. Note that we can easily adjust the formula to give the price of the Call option at any date $t \leq T$.

3 Dynamics of the VXX

3.1 Introducing the VXX

The introduction by CBOE of VIX futures in 2004 and VIX options in 2006 provided market players with tools to trade the implied volatility of the S&P 500 in a direct manner. Typically, VIX futures may be used not only for hedging positions on options on the S&P 500 or the VIX but also to hedge positions on S&P 500 futures and, more generally, positions on the equity market, as the VIX index is negatively correlated with the S&P 500. Yet, as discussed in Section 1, some features of VIX futures and options may hinder its access by non institutional investors.

For example, as of March 2018, each VIX futures contract is written on a nominal value of around \$18,500, the VIX being around 18.5, and the minimum price increment is \$50 per contract, which is remarkably large (in absolute value) compared to stocks. A way to benefit from lower price increments is to trade VIX futures by blocks. The minimum block size is 200 contracts, i.e. \$3,700,000 nominal value and the price increment is reduced to \$5 per contract, which is still significantly larger than what is encountered in equity markets.

Another issue that arises when trading VIX futures is liquidity and roll-over risk. The liquidity of VIX futures is generally a decreasing function of the maturity of the contract: the longer the contract

maturity, the larger the bid-ask spread and the lower the volumes exchanged for that contract. As a consequence, many market players prefer to take positions on the VIX futures with nearest expiry. Hence, if they want to keep such positions after the futures with nearest expiry comes to maturity, they need to roll-over their position to the next available maturity. By doing so, they are exposed to a roll-over risk, that is the risk that the futures price for the next maturity may be unfavorable compared to the futures price with nearest maturity.

Those limitations on the VIX futures market motivated the introduction of a new class of instruments related to the VIX: exchange-traded notes (ETNs) on the VIX. An ETN is an unsecured and unsubordinated debt security whose returns are based on the performance of an index (minus applicable fees). Contrary to exchange-traded funds which are backed by a basket of assets, owning an ETN is different from owning interests in the index that it tracks or in a security that is linked to the performance of the index. Investors in an ETN rather receive the tracked return as long as the issuer of the ETN is able to deliver it, which naturally makes the ETN sensitive to the credit risk of its issuer.

In January 2009, Barclays launched two ETNs on the VIX: the VXX and the VXZ. In this paper we study the VXX in detail as it is the most traded ETN on the VIX, with a remarkable growth of volumes over the last years. The VXX is designed so as to track the performance of a synthetic 30-day futures contract on the VIX. To achieve that, Barclays implemented a formula for the VXX return which is equal to a combination of returns of two (traded) VIX futures, offering a “daily rolling long position in the first and second month VIX futures contracts” (Barclays, 2016). In that sense, the computation of the VXX, which is based on two VIX futures with maturities straddling a 30-day maturity, is similar to that of the VIX itself, calculated from S&P 500 option prices with maturities straddling a fixed 30-day time frame.

Denote I_t the value of the VXX at date t and $F(t, T)$ the VIX futures price with expiry T . The return of the VXX between dates t and $t + 1$ is given by

$$\frac{I_{t+1} - I_t}{I_t} = r + \frac{a(t)(F(t+1, T_1) - F(t, T_1)) + (1 - a(t))(F(t+1, T_2) - F(t, T_2))}{a(t)F(t, T_1) + (1 - a(t))F(t, T_2)} \quad (7)$$

where T_1 is the nearest month expiry, T_2 is the second next-month expiry, $a(t) = \frac{T_1-t}{T_2-T_1}$ is the rolling factor and r is an interest rate indexed on US Treasury bills.

Remark that $a(t)(T_1-t) + (1-a(t))(T_2-t) = 30$ days, which explains that the VXX tracks a 30-day VIX futures. VXX is traded on NYSE ARCA and has the same advantages as stocks: small denominations (as of March 2018, its value is around \$42), small bid-ask spreads and large traded volumes (figure). In addition, as it offers a rolling exposure to VIX futures with maturities T_1 and T_2 , it smoothes the roll-over risk.

Whereas VXX is designed to track a 30-day VIX futures, its past performance has been remarkably poor compared to that of the VIX itself, as seen in Figure 1. Intuitively, this can be explained by Equation (7): everyday, the VXX offers an increased (resp. reduced) exposure to the future contract with maturity T_2 (resp. T_1). This implies a daily rolling cost for the VXX when the VIX futures term structure is in contango (i.e. increasing). Note that, symmetrically, the VXX benefits from a term-structure which is in backwardation. In practice, the performance of the VXX has been so poor that it had to undergo 5 reverse splits (each time with a 1:4 ratio) in less than 9 years, in order to keep its price away from zero. Yet, volumes on the VXX are larger than ever as the VXX enables investors to get a cheap and liquid exposure on the implied volatility of the S&P 500.

3.2 Dynamics of the VXX

From the pricing supplement of the VXX Prospectus of Barclays we get that the dynamics of the VXX, denoted I_t throughout the paper, is given by

$$\frac{dI_t}{I_t} = rdt + \frac{a(t)dF(t, T_1) + (1 - a(t))dF(t, T_2)}{a(t)F(t, T_1) + (1 - a(t))F(t, T_2)}, \quad (8)$$

where $F(t, T_i), i = 1, 2$ are given by Proposition 2.1 and the deterministic function $a(t)$ is defined as follows:

$$a(t) = \frac{T_2 - (t + \tau)}{T_2 - T_1} = \frac{T_1 - t}{T_2 - T_1} \quad (9)$$

with $\tau = T_2 - T_1$ the constant rolling maturity (equal to 30 days in the case of VXX).

Using Equation 5, we find that

$$\frac{dI_t}{I_t} = rdt + \sigma\sqrt{\alpha X_t + \beta}dZ_t + \omega \frac{a(t)F(t, T_1)\Psi(t, T_1) + (1 - a(t))F(t, T_2)\Psi(t, T_2)}{a(t)F(t, T_1) + (1 - a(t))F(t, T_2)}\sqrt{\alpha X_t + \beta}dW_t \quad (10)$$

which, given Equation (1), can be rewritten as

$$\frac{dI_t}{I_t} = \frac{dS_t}{S_t} + \delta X_t dt + \omega \frac{a(t)F(t, T_1)\Psi(t, T_1) + (1 - a(t))F(t, T_2)\Psi(t, T_2)}{a(t)F(t, T_1) + (1 - a(t))F(t, T_2)}\sqrt{\alpha X_t + \beta}dW_t. \quad (11)$$

In Equation (1), we see that the term δX_t drives the term structure of VIX futures prices. In particular, when $\delta X_t < 0$, VIX futures prices are in contango and equation (11) shows that the term δX_t captures the systematic loss of the VXX in that case.

The definition of the VXX given in (7) is used in practice by Barclays as it makes the VXX replicable through a self-financing portfolio composed of VIX futures with maturities T_1 and T_2 , hence giving the opportunity to Barclays to hedge its VXX issuances. A theoretical 30-day maturity VIX futures should rather be given by

$$a(t)F(t, T_1) + (1 - a(t))F(t, T_2) \quad (12)$$

which is however non investable (Galai, 1979). As done in Alexander and Korovilas (2013), we can hence define the rolling cost of the ETN as the difference between its return and the return of the theoretical and non-tradable benchmark. In the case of the VXX, this rolling cost can be written

$$\begin{aligned} \frac{dI_t}{I_t} - \left(rdt + \frac{d(a(t)F(t, T_1) + (1 - a(t))F(t, T_2))}{a(t)F(t, T_1) + (1 - a(t))F(t, T_2)} \right) \\ = \frac{F(t, T_1) - F(t, T_2)}{(T_2 - T_1)(a(t)F(t, T_1) + (1 - a(t))F(t, T_2))} \end{aligned}$$

which is clearly negative (systematic loss) whenever the term-structure of the VIX is in contango. In addition, the steeper the VIX futures term-structure between maturities T_1 and T_2 , the larger the rolling cost for the ETN. In practice, the VIX term structure exhibits, most of the times, steep contango in the short-end while the long-end is more flat. This explains why rolling costs for the VXX, which is built with futures with one and two months maturities, are usually larger than that of ETNs tracking longer-term VIX maturities, such as the VXZ which is built with a stream of futures with maturities four to seven months.

4 Spot volatility developments

While our framework enables to model VIX and VXX in a consistent manner – which, among other things, enables to quantify the systematic loss of VXX when VIX is in contango –, the complex dynamics of VXX (see Equation (10)) makes it difficult to link, in a tractable manner, the volatility/skew properties of the VXX to that of the VIX. In this section, we somehow try to quantify the spot volatility/skew of the VXX and establish a link with the VIX. To that end, we perform an expansion of VIX and VXX with respect to the parameter ω .

The main conclusion of this section is that, as long as we stick to the simplistic case where $\omega = 0$, VIX and VXX have the same spot volatility/skew properties. However, when considering order 1 (and above) in ω , we find that spot volatility/skew of VXX can differ significantly from that of VIX and, more interestingly, that the difference is driven by a stochastic process. This is in line, and quantifies, a well-known fact in the VXX market, which is that the observation of only VIX volatility/skew is insufficient to deduce the volatility/skew of VXX.

4.1 Order zero in ω

We first consider the zero-order development in ω . This means that we take $\omega = 0$ in the formulae. We denote by \bar{X}_t the process (2) with $\omega = 0$, that is the deterministic process satisfying

$$dX_t = \kappa(\theta - X_t)dt,$$

therefore

$$\bar{X}_t = \theta + (X_0 - \theta)e^{-\kappa t}.$$

Now consider the VIX dynamics corresponding to the process \bar{X}_t :

$$\frac{d\bar{S}_t}{\bar{S}_t} = (r - \delta\bar{X}_t)dt + \sigma\sqrt{\alpha\bar{X}_t + \beta}dZ_t, \quad \bar{S}_0 > 0,$$

then it follows easily that the futures price is given by

$$\bar{F}(t, T) = \bar{S}_t e^{r(T-t) - \delta \int_t^T \bar{X}_s ds} \quad (13)$$

$$= \bar{S}_t e^{\bar{\Phi}(t, T) + \bar{X}_t \bar{\Psi}(t, T)}, \quad (14)$$

where the functions $\bar{\Psi}, \bar{\Phi}$ are given by

$$\begin{aligned} \bar{\Psi}(t, T) &= -\frac{\delta}{\kappa} \left(1 - e^{-\kappa(T-t)} \right), \\ \bar{\Phi}(t, T) &= (r - \delta\theta)(T - t) + \frac{\delta\theta}{\kappa} \left(1 - e^{-\kappa(T-t)} \right). \end{aligned}$$

In the case $\omega = 0$, (5) can be written:

$$\frac{dF(t, T)}{F(t, T)} = \sigma\sqrt{\alpha\bar{X}_t + \beta}dZ_t,$$

which implies the following dynamics for the VXX:

$$\begin{aligned} \frac{dI_t}{I_t} &= rdt + \frac{a(t)dF(t, T_1) + (1 - a(t))dF(t, T_2)}{a(t)F(t, T_1) + (1 - a(t))F(t, T_2)} \\ &= rdt + \sigma\sqrt{\alpha\bar{X}_t + \beta}dZ_t. \end{aligned}$$

Thus, at the order zero in ω the volatility of VXX coincides with the one of VIX (and VIX futures).

4.2 Order one in ω

Let us now consider the development of the volatility and the skew of the VXX at order 1 in ω . First we have to consider the order zero of the following term:

$$\frac{a(t)F(t, T_1)\Psi(t, T_1) + (1 - a(t))F(t, T_2)\Psi(t, T_2)}{a(t)F(t, T_1) + (1 - a(t))F(t, T_2)} \sqrt{\alpha X_t + \beta}.$$

which, from (14), is equal to:

$$\frac{a(t)\bar{F}(t, T_1)\bar{\Psi}(t, T_1) + (1 - a(t))\bar{F}(t, T_2)\bar{\Psi}(t, T_2)}{a(t)\bar{F}(t, T_1) + (1 - a(t))\bar{F}(t, T_2)} \sqrt{\alpha\bar{X}_t + \beta},$$

Notice that the previous expression is deterministic as the terms \bar{S}_t simplify.

In conclusion, the term of order 1 in ω in the diffusion term of the VXX is given by

$$\frac{dI_t}{I_t} = \dots + \omega \frac{a(t)\bar{F}(t, T_1)\bar{\Psi}(t, T_1) + (1 - a(t))\bar{F}(t, T_2)\bar{\Psi}(t, T_2)}{a(t)\bar{F}(t, T_1) + (1 - a(t))\bar{F}(t, T_2)} \sqrt{\alpha\bar{X}_t + \beta} dW_t + o(\omega).$$

Let us now focus on the first order term in ω of the volatility term $\sigma\sqrt{\alpha X_t + \beta}$ in the VIX dynamics. Let us write X_t as

$$X_t = \bar{X}_t + \omega Y_t + o(\omega), \quad (15)$$

so that

$$\sigma\sqrt{\alpha X_t + \beta} = \sigma\sqrt{\alpha \bar{X}_t + \beta + \omega\alpha Y_t + o(\omega)}.$$

Now

$$dX_t = d\bar{X}_t + \omega dY_t,$$

and from the dynamics of X_t (2) we get

$$\kappa(\theta - X_t)dt + \omega\sqrt{\alpha X_t + \beta}dW_t = \kappa(\theta - \bar{X}_t)dt + \omega dY_t,$$

so that

$$\begin{aligned} \omega\sqrt{\alpha X_t + \beta}dW_t &= \kappa(X_t - \bar{X}_t)dt + \omega dY_t \\ &= \kappa\omega Y_t + \omega dY_t, \end{aligned}$$

that is Y_t satisfies the SDE

$$dY_t + \kappa Y_t = \sqrt{\alpha X_t + \beta}dW_t.$$

At order 0 in ω it becomes

$$dY_t + \kappa Y_t = \sqrt{\alpha \bar{X}_t + \beta}dW_t,$$

whose solution is given by

$$Y_t = e^{-\kappa t} \int_0^t e^{\kappa s} \sqrt{\alpha \bar{X}_s + \beta} dW_s.$$

In conclusion we can write the volatility term of the VIX as follows:

$$\sigma\sqrt{\alpha X_t + \beta} = \sigma\sqrt{\alpha \bar{X}_t + \beta} \left(1 + \omega \frac{\alpha Y_t}{2(\alpha \bar{X}_t + \beta)} + o(\omega) \right).$$

We can now compute the term of order 1 in ω of the VXX dynamics:

$$\frac{dI_t}{I_t} = rdt + \sigma\sqrt{\alpha \bar{X}_t + \beta} \left(1 + \omega \frac{\alpha Y_t}{2(\alpha \bar{X}_t + \beta)} + o(\omega) \right) dZ_t \quad (16)$$

$$+ \omega \frac{a(t)\bar{F}(t, T_1)\bar{\Psi}(t, T_1) + (1-a(t))\bar{F}(t, T_2)\bar{\Psi}(t, T_2)}{a(t)\bar{F}(t, T_1) + (1-a(t))\bar{F}(t, T_2)} \sqrt{\alpha \bar{X}_t + \beta} dW_t + o(\omega). \quad (17)$$

Remark 4.1. Due to the presence of the stochastic term Y_t in the volatility, we expect an impact on the skew in VIX and VXX at the first order in ω .

Let us denote

$$c(t) = \frac{a(t)\bar{F}(t, T_1)\bar{\Psi}(t, T_1) + (1-a(t))\bar{F}(t, T_2)\bar{\Psi}(t, T_2)}{a(t)\bar{F}(t, T_1) + (1-a(t))\bar{F}(t, T_2)}.$$

Then, at the order 1 in ω , the instantaneous variance is given by:

$$Var_I = \sigma^2(\alpha \bar{X}_t + \beta) + \omega\alpha\sigma^2 Y_t + 2\sigma(\alpha \bar{X}_t + \beta)\omega c(t)\rho + o(\omega), \quad (18)$$

where the only stochastic term is the one involving Y_t .

4.3 Skew of VXX

From (17) and (18) we get

$$\begin{aligned}\left\langle \frac{dI_t}{I_t}, dVar_I \right\rangle &= \rho \sigma^3 \alpha \omega (\alpha \bar{X}_t + \beta) dt + o(\omega), \\ \left\langle \frac{dI_t}{I_t} \right\rangle &= \sigma^2 (\alpha \bar{X}_t + \beta) \left(1 + \omega \left(\frac{\alpha Y_t}{\alpha \bar{X}_t + \beta} + \frac{2\rho c(t)}{\sigma \sqrt{\alpha \bar{X}_t + \beta}} \right) \right) dt + o(\omega), \\ \langle dVar_I \rangle &= \omega^2 \alpha^2 \sigma^4 (\alpha \bar{X}_t + \beta) dt.\end{aligned}$$

We have now all the ingredients to compute the skew of the VXX:

$$\begin{aligned}\left\langle \frac{dI_t}{I_t}, dVar_I \right\rangle &= \\ Skew &= \frac{\rho \sigma^3 \alpha \omega (\alpha \bar{X}_t + \beta)}{\sigma \sqrt{\alpha \bar{X}_t + \beta} \left(1 + \omega \left(\frac{\alpha Y_t}{\alpha \bar{X}_t + \beta} + \frac{2\rho c(t)}{\sigma \sqrt{\alpha \bar{X}_t + \beta}} \right) \right)^{1/2} \omega \alpha \sigma^2 \sqrt{\alpha \bar{X}_t + \beta}} \\ &= \frac{\rho}{\left(1 + \omega \left(\frac{\alpha Y_t}{\alpha \bar{X}_t + \beta} + \frac{2\rho c(t)}{\sigma \sqrt{\alpha \bar{X}_t + \beta}} \right) \right)^{1/2}} \\ &= \rho \left(1 - \frac{\omega}{2} \left(\frac{\alpha Y_t}{\alpha \bar{X}_t + \beta} + \frac{2\rho c(t)}{\sigma \sqrt{\alpha \bar{X}_t + \beta}} \right) \right) + o(\omega).\end{aligned}$$

Notice that at the order 0 in ω the skew is equal to the constant ρ . At the order 1, we have a term structure of the implied volatility and a stochastic skew.

5 Option pricing and implied volatility

We now focus on the implied volatility and option prices for the VXX. Similarly as in the previous section, given the complex dynamics followed by the VXX (see Equation (10)), we cannot obtain analytical formulas for VXX option prices in the general case and we study here some developments of options prices.

5.1 Order 0 in ω

At order 0 in ω , (11) implies that:

$$\frac{I_T}{I_0} = \frac{S_T}{S_0} \exp(\bar{\delta}T)$$

where

$$\bar{\delta} = \frac{1}{T} \int_0^T \delta \bar{X}_t dt$$

The price of a Call option written on the VXX, with maturity T and (percentage) strike k is given by

$$\begin{aligned}C_I(T, k) &= e^{-rT} \mathbb{E} [(I_T - kI_0)_+] \\ &= e^{-rT} \mathbb{E} \left[\left(\frac{S_T}{S_0} I_0 e^{\bar{\delta}T} - kI_0 \right)_+ \right] \\ &= \frac{I_0}{S_0} e^{\bar{\delta}T} e^{-rT} \mathbb{E} \left[(S_T - kS_0 e^{-\bar{\delta}T})_+ \right],\end{aligned}$$

which enables to make a link between the price of a Call on the VXX and that of a Call on the VIX:

$$\frac{1}{I_0} C_I(T, k) = \frac{1}{S_0} e^{\bar{\delta}T} C_S(T, ke^{-\bar{\delta}T}). \quad (19)$$

The price of the Call option on the VXX with strike k can hence be deduced from the (scaled) price of a Call option on the VIX, but with equivalent strike $ke^{-\bar{\delta}T}$.

In practice, Call options on VIX are quoted in terms of Black and Scholes volatility. We denote the price, at date 0, of a Call option written on an underlying P , with maturity T , (percentage) strike k , implied volatility v and dividend yield q by:

$$C_{B\&S}(P_0, T, k, v, q).$$

Denote by $v_S(T, k)$ the VIX volatility surface and $v = v_S(T, ke^{-\bar{\delta}T})$. We can hence write:

$$C_S(T, ke^{-\bar{\delta}T}) = C_{B\&S}(S_0, T, ke^{-\bar{\delta}T}, v, 0) = S_0 \mathcal{N}(d_1) - k S_0 e^{-\bar{\delta}T} e^{-rT} \mathcal{N}(d_2),$$

where \mathcal{N} is the cumulative probability distribution of a standard Gaussian random variable and:

$$d_1 = \frac{1}{v\sqrt{T}} \left[\ln \left(\frac{S_0}{k S_0 e^{-\bar{\delta}T}} \right) + \left(r + \frac{v^2}{2} \right) T \right] = \frac{1}{v\sqrt{T}} \left[\ln \left(\frac{I_0}{k I_0} \right) + \left(r + \bar{\delta} + \frac{v^2}{2} \right) T \right],$$

$$d_2 = d_1 - v\sqrt{T}.$$

Given (19), we find that:

$$C_I(T, k) = I_0 e^{\bar{\delta}T} \mathcal{N}(d_1) - k I_0 e^{-rT} \mathcal{N}(d_2), \quad (20)$$

which means that the price of the Call option on the VXX with strike k can be calculated using the Black and Scholes formula with dividend yield $-\bar{\delta}$ and adjusted implied volatility of the VIX $v = v_S(T, ke^{-\bar{\delta}T})$:

$$C_I(T, k) = C_{B\&S}(I_0, T, k, v_S(T, ke^{-\bar{\delta}T}), -\bar{\delta}). \quad (21)$$

In practice, the VXX does not pay any dividend and the market prices options on the VXX using the Black & Scholes implied volatility surface of the VXX, $v_I(T, k)$, and no dividends. This leads to the following equality:

$$C_I(T, k) = C_{B\&S}(I_0, T, k, v_I(T, k), 0) = C_{B\&S}(I_0, T, k, v_S(T, ke^{-\bar{\delta}T}), -\bar{\delta}),$$

which characterizes the implied volatility surface of the VXX from that of the VIX.

Remark that when $\bar{\delta} = 0$, $v_I(T, k) = v_S(T, k)$ and using the implicit function theorem, it is possible to develop (21) for $\bar{\delta} \ll 1$:

$$v_I(T, k) = v_S(T, k) - \frac{\bar{\delta}}{\frac{\partial C_{B\&S}}{\partial v}} \left(\frac{\partial C_{B\&S}}{\partial \bar{\delta}} + kT \frac{\partial C}{\partial v} \frac{\partial v_S}{\partial k} \right) + o(\bar{\delta})$$

and find the link between the skew of the VXX (namely $\frac{\partial v_I}{\partial k}$) and that of the VIX (related with $\frac{\partial v_S}{\partial k}$) by deriving (21) with respect to k :

$$\frac{\partial C_{B\&S}}{\partial k}(\bar{\delta} = 0) + \frac{\partial C_{B\&S}}{\partial v} \frac{\partial v_I}{\partial k} = \frac{\partial C_{B\&S}}{\partial k}(\bar{\delta}) + e^{-\bar{\delta}T} \frac{\partial C_{B\&S}}{\partial v} \frac{\partial v_S}{\partial k}.$$

5.2 A Black-Scholes type approximation for the VXX

In this section we adopt the simplification suggested by Bergomi (2016) (see Formula (7.94)), where the original dynamics of the prospectus (8) is replaced by the following one:

$$\frac{dI_t}{I_t} = rdt + a(t) \frac{dF(t, T_1)}{F(t, T_1)} + (1 - a(t)) \frac{dF(t, T_2)}{F(t, T_2)}. \quad (22)$$

We introduce an additional simplification by taking $\alpha = 0$, which means that the dynamics of the futures (5) becomes

$$\frac{dF(t, T)}{F(t, T)} = \sigma \sqrt{\beta} dZ_t + \omega \Psi(t, T) \sqrt{\beta} dW_t, \quad (23)$$

where the function $\Psi(t, T)$ takes the form

$$\Psi(t, T) = -\frac{\delta}{\kappa} \left(1 - e^{-\kappa(T-t)} \right). \quad (24)$$

The VXX dynamics becomes

$$\frac{dI_t}{I_t} = rdt + \sigma\sqrt{\beta}dZ_t + \frac{\omega\delta\sqrt{\beta}}{\kappa} (\gamma(t) - 1) dW_t, \quad (25)$$

where the deterministic function $\gamma(t)$ is given by

$$\gamma(t) = a(t)e^{-\kappa(T_1-t)} + (1-a(t))e^{-\kappa(T_2-t)}. \quad (26)$$

It follows that under such specification the VXX is log-normally distributed

$$\ln I_t \approx \mathcal{N} \left(rt - \frac{1}{2} \langle \ln I \rangle_t; \langle \ln I \rangle_t \right), \quad (27)$$

where the variance is given by

$$\begin{aligned} \langle \ln I \rangle_t &= \sigma^2 \beta t + \frac{\omega^2 \delta^2 \beta}{\kappa^2} \int_0^t (\gamma(s) - 1)^2 ds + 2 \frac{\sigma \omega \delta \beta \rho}{\kappa} \int_0^t (\gamma(s) - 1) ds \\ &= \left(\sigma^2 + \frac{\omega^2 \delta^2}{\kappa^2} - 2 \frac{\sigma \omega \delta \rho}{\kappa} \right) \beta t + 2 \left(\frac{\sigma \omega \delta \rho}{\kappa} - \frac{\omega^2 \delta^2}{\kappa^2} \right) \beta \int_0^t \gamma(s) ds + \frac{\omega^2 \delta^2 \beta}{\kappa^2} \int_0^t \gamma^2(s) ds. \end{aligned}$$

In Appendix 9.5 we provide the explicit expression for the integrals $\int_0^t \gamma(s) ds$ and $\int_0^t \gamma^2(s) ds$. In order to price a call option on the VXX when $\alpha = 0$ we can then use the Black-Scholes formula giving:

$$Call_{VXX}(t, T, K) = I_t \mathcal{N}(d_1) - e^{-r(T-t)} K \mathcal{N}(d_2),$$

where T denotes the maturity of the option, K is the strike and d_1 is given by

$$d_1 = \frac{\ln \left(\frac{I_t}{K} \right) + r(T-t) + \frac{1}{2} \langle \ln I \rangle_{T-t}}{\sqrt{\langle \ln I \rangle_{T-t}}}. \quad (28)$$

6 Numerical illustration

In this subsection we display some features of our model. In particular we show its flexibility in reproducing the stylized facts of the VIX futures and option markets.

6.1 The term structures of futures prices

Let's consider the one factor specification of the model given by (2) and (1). The first object is to be able to reproduce a good fit of the term structure of the futures prices. This is particularly important in view of pricing ETNs on the VIX that explicitly depend on futures prices on the VIX. Looking at the dynamics (1), one can guess that the contango/backwardation effects of the term structure of futures prices are controlled by the sign of the parameter δ . This is indeed the case: using the closed form formula (62) for futures prices on the VIX, we fix a set of parameters and let δ vary. The left hand side of Figure (3) reproduces a term structure in contango and is obtained with a negative $\delta = -0.1$, while in the right hand side we get a term structure in backwardation with the same parameters but with a positive $\delta = 0.1$. The other parameters are fixed as follows: $X_0 = 0.1, S_0 = 20, \omega = 1, \kappa = 0.9, \theta = 1.11, \alpha = 0, \beta = 1, \rho = 0.5, r = 0, \sigma = 0.4$.

The case of a humped term structure is more subtle, but it can still be handled quite easily within the model. For example, one could introduce an additional constant term $\bar{\delta}$ in the mean reversion of the VIX process as follows:

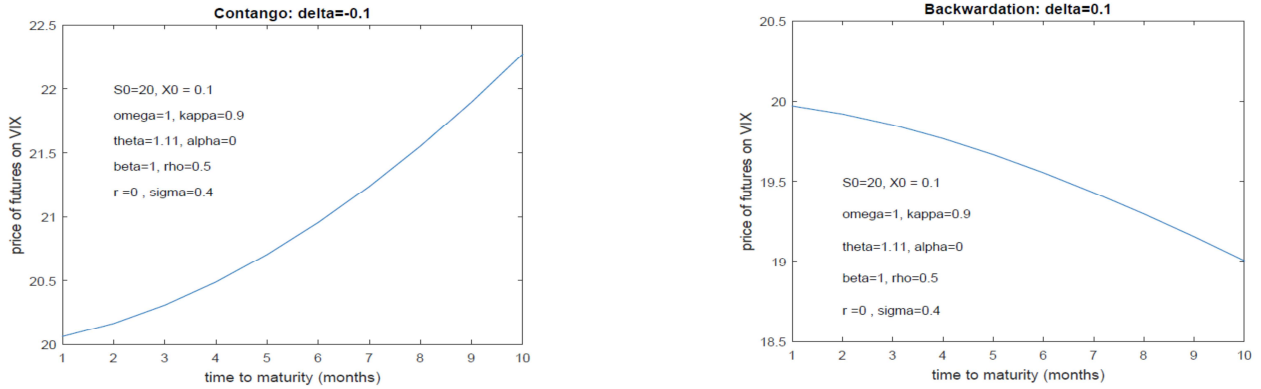


Figure 3: Left: generating a term structure of futures prices in contango with a negative $\delta = -0.1$; Right: generating a term structure of futures prices in backwardation with a positive $\delta = 0.1$. The other parameters are fixed as follows: $X_0 = 0.1, S_0 = 20, \omega = 1, \kappa = 0.9, \theta = 1.11, \alpha = 0, \beta = 1, \rho = 0.5, r = 0, \sigma = 0.4$.

$$\frac{dS_t}{S_t} = (r + \bar{\delta} - \tilde{\delta}Y_t)dt + \tilde{\sigma}\sqrt{Y_t}dZ_t, \quad (29)$$

$$dY_t = \tilde{\kappa}(\tilde{\theta} - Y_t)dt + \tilde{\omega}\sqrt{\tilde{\alpha}Y_t + \tilde{\beta}}dW_t \quad (30)$$

which is of course equivalent to the initial dynamics (1) modulo the change in the parametrization $Y_t = X_t + \bar{\delta}/\delta, \tilde{\delta} = \delta, \tilde{\sigma} = \sigma, \tilde{\alpha} = \alpha, \tilde{\beta} = \beta - \alpha\bar{\delta}/\delta, \tilde{\theta} = \theta + \bar{\delta}/\delta, \tilde{\kappa} = \kappa$. However, the latter is preferred as it revealed to be more stable in the empirical calibrations, especially in the case $X_0 < 0$ ¹. In Figure 4 we generate a humped term structure of futures prices with positive $\bar{\delta} = 1$ and $\tilde{\delta} = 0.5$. The corresponding parameters in the original specification (1) are fixed as follows: $X_0 = -1, S_0 = 20, \omega = 1, \kappa = 0.1, \theta = 13, \alpha = 0, \beta = 1, \rho = 0.5, r = 0, \sigma = 0.4$.

6.2 Loss in contango

The second effect that we would like to be able to reproduce is the under-performance of the VXX with respect to the VIX when the term structure of futures is in contango. This is clear when looking at the Equation (11), where we see that in the case of contango, i.e. when δ is negative, the difference between the VXX and VIX returns involves a negative term in the drift, plus a martingale term that is zero in average. A Monte Carlo exercise confirms the typical loss in contango also in our model. We simulate the trajectories of the VXX and VIX processes for $\delta = -0.1$ and we generate Figure 5, where we have normalized the prices of VIX and VXX at 100 and the beginning of the period and we plot the average difference between them. We clearly see that the VIX over-performs the VXX.

6.3 The VIX implied volatility surface

Our model is flexible enough to reproduce different behaviors of the implied volatility surface on the VIX. We consider the implied volatility surface generated by the model for the parameter set associated to the term structure in contango and backwardation, assuming that there are 10 maturities (1,2,...,10 months) and strikes ranging between 80% and 120% of the futures price, corresponding to the same maturity

¹Another possibility consists in introducing a 2-factor specification of the model, so that one can play with δ_1, δ_2 in order to reproduce a humped term structure. This choice introduces a great flexibility in the model, at the cost of an important number of parameters to be calibrated.

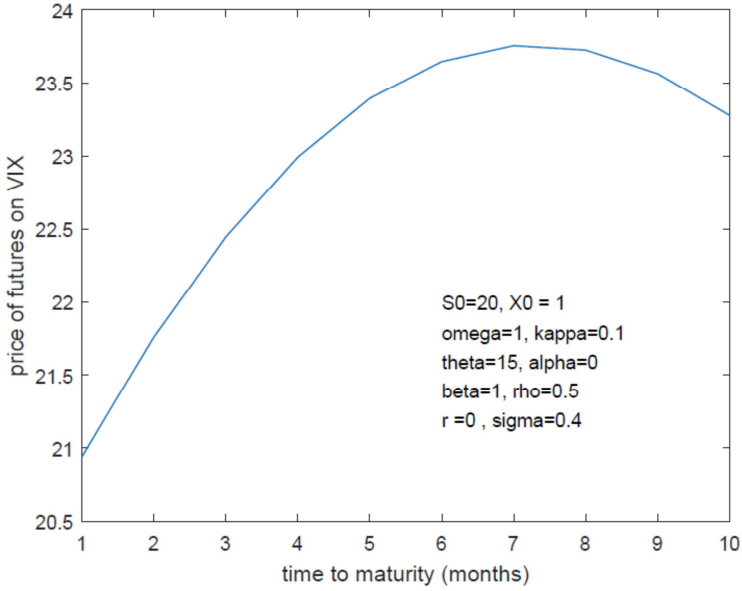


Figure 4: Generating a humped term structure of futures prices with a $\bar{\delta} = 1$ and $\tilde{\delta} = 0.5$. The corresponding parameters in the original specification are fixed as follows: $X_0 = -1, S_0 = 20, \omega = 1, \kappa = 0.1, \theta = 13, \alpha = 0, \beta = 1, \rho = 0.5, r = 0, \sigma = 0.4$.

of the option. Prices are obtained through the FFT procedure according to the formulas developed in Subsection 2.

As we see in Figure 6, the model is able to generate both increasing concave and decreasing convex smiles. In the left hand side (resp. right hand side) of Figure 6 there is the implied volatility surface corresponding to the term structure of futures in contango (resp. in backwardation).

6.4 The VXX implied volatility surface

In this subsection we provide the implied volatility surface for VXX vanilla options generated by our model under different conditions of the term structure of VIX futures. In order to get option prices on the VXX, we will perform a Monte Carlo simulation, as the VXX process does not satisfy any analytical property, in particular the VXX process is not affine.

Figure 7 shows that the implied volatility surface for the VXX is similar to the one generated for the VIX, according to the particular term structure of the futures on VIX.

7 Calibration results on real data

In this section we will first show the performance of our model in calibrating real data on futures prices and vanillas on VIX. Next, once calibrated the model using inputs only from the VIX market, we shall see that the implied volatility surface for the VXX generated by the calibrated model is very close to the one quoted in the market. This out-of-sample result constitutes the main empirical contribution of the paper.

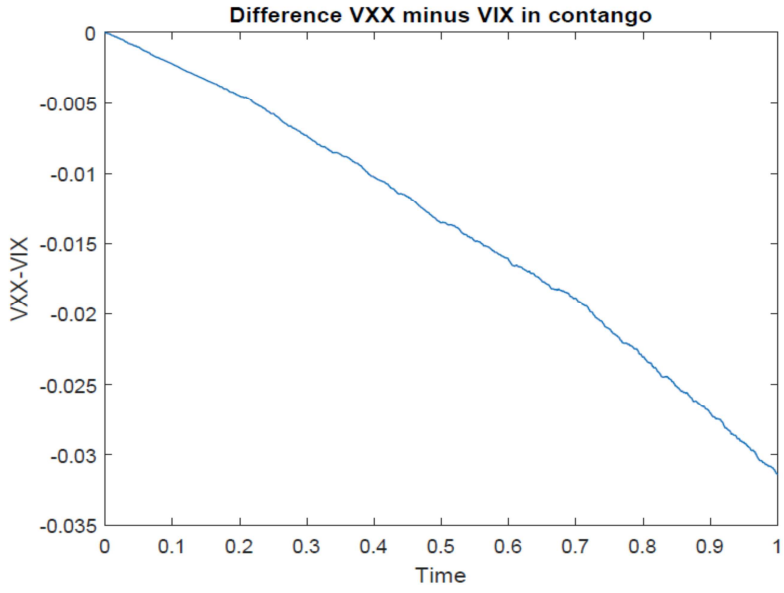


Figure 5: Difference between the (normalized) VXX and VIX values when the term structures of futures on VIX is in contango, corresponding to the case $\delta = -0.1$. The other parameters are fixed as follows: $X_0 = 0.1$, $S_0 = 20$, $\omega = 1$, $\kappa = 0.9$, $\theta = 1.11$, $\alpha = 0$, $\beta = 1$, $\rho = 0.5$, $r = 0$, $\sigma = 0.4$.

7.1 Calibration on futures and options on VIX

We consider two trading dates: the 16th December 2015, when the term structure of futures prices of VIX was in contango, and the 21th January 2016 when it was in backwardation.

The input data for the calibration available from a major provider are the futures montly prices (available for 8 maturities) and the implied volatilities corresponding to 1,3 and 6 months, with moneyness (in term of ratio between futures prices and strike) ranging from 80% to 120%, for a total of 21 option volatilities and 8 futures prices.

Figure 8 shows the results of the calibration for the 16th December 2015, when the term structure of the futures prices was in contango. Overall the fit is quite good, compared with the typical performance of a one-factor Heston-based model like ours.

In order to improve the fit, one can adopt a two-factor specification of the model as follows:

$$\frac{dS_t}{S_t} = (r + \bar{\delta} - \tilde{\delta}_1 Y_{1t})dt + \tilde{\sigma}_1 \sqrt{Y_{1t}} dZ_{1t} + \tilde{\sigma}_2 \sqrt{Y_{2t}} dZ_{2t}, \quad (31)$$

where the factors Y_{it} , $i = 1, 2$ follow two independent CIR dynamics as in (30). Figure 9 illustrates the fit of the two-factor specification of the model for market data as on Dec. 16, 2015, where the VIX value was 17,86%. We note that the fit has been improved by the introduction of the second factor. Although the high number of parameters to be calibrated does not justify the added value of the 2-factor specification of the model in a pure calibration perspective of the VIX market, we shall see in the next section that adding a second factor may be important if we are mostly interested in the ETN market as well.

Next, we consider the case of data as on Jan. 19, 2016, where the term structure of futures prices on VIX was in backwardation.

Figure 10 shows that the model is flexible enough to fit relatively well also a term structure in backwardation, as for the 21th January 2016, together with the corresponding implied volatility surface.

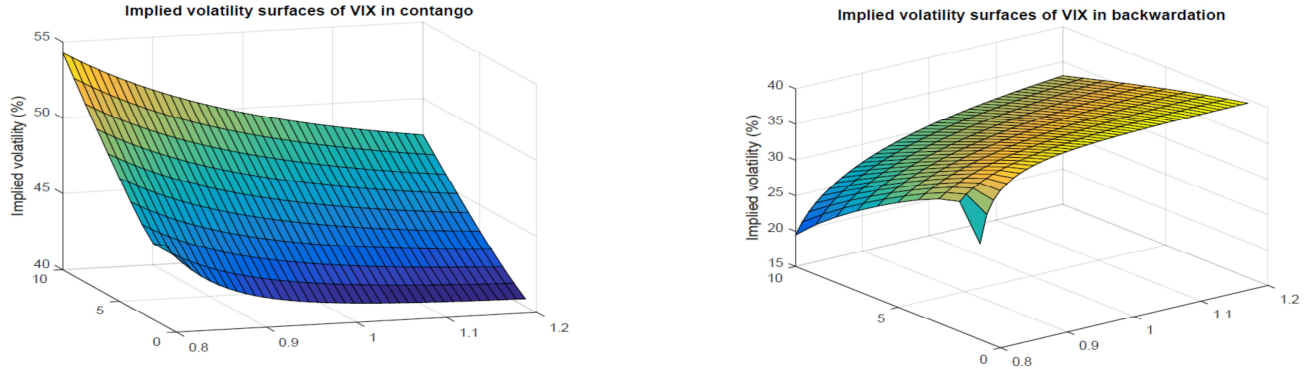


Figure 6: Left: implied volatility surface for VIX generated when the term structure of futures prices is in contango with a negative $\delta = -0.1$; Right: implied volatility surface for VIX generated when the term structure of futures prices is in backwardation with a positive $\delta = 0.1$. The other parameters are fixed as follows: $X_0 = 0.1, S_0 = 20, \omega = 1, \kappa = 0.9, \theta = 1.11, \alpha = 0, \beta = 1, \rho = 0.5, r = 0, \sigma = 0.4$. Strikes range between 80% and 120% of the corresponding futures price. Maturities range between 1 and 10 months.

7.2 Out of sample fit of the VXX implied volatility surface

We have now all the ingredients to test the consistency of our approach. We produce the VXX option prices and implied volatilities through a Monte Carlo simulation using formulas introduced in Subsection 3.2 and we compare the results with market data for the two trading days considered in the previous subsection.

First we consider the implied volatility curves at 1, 3, 6 months for the VXX as on Dec 16, 2015, where the VXX value was 19,34% and the term structure of futures on VIX was in contango. Figures 11, 12, 13 show the results of the fit of the VXX implied volatility smiles for the one factor specification of our calibrated model. The results are quite good, mostly if we take into account that the fit for the VXX market is completely out-of-sample. We also display the fit of the VIX smiles obtained by a Monte Carlo simulation of the calibrated model as a double check.

We can even increase the quality of the fit of the VXX smiles by adding a second factor in the specification of our model. Figures 14, 15, 16 show the results of the fit, which is now excellent.

Finally, we consider the implied volatility curves at 1, 3, 6 months for the VXX as on Jan 21, 2016, where the VXX value was 27,29% and the term structure of futures on VIX was in backwardation. Here the results for the VXX are good already in the one factor specification of the model. In conclusion, VXX prices generated by our calibrated model are in line with market quotes, thus proving the consistency of our framework.

8 Conclusion

This paper develops a quantitative framework for modeling VIX and VXX in a consistent manner. The benchmark model used for the VIX is flexible enough to yield closed form formulas for VIX derivatives and sophisticated enough to reproduce the empirical features observed on the VIX (varying term-structure of futures prices, smile and skew of VIX options). It enables to link the properties of the VXX (drift, implied volatility of VXX options, smile/skew of VXX options) to the factors underlying the VIX dynamics in a tractable manner. As such it gives an intuition about the joint behavior of VIX and VXX and enables to anticipate systematic effects on the VXX from the VIX dynamics. Our approach can be used for modelling any exchange-traded note on the VIX in relation to the VIX itself and is particularly useful for

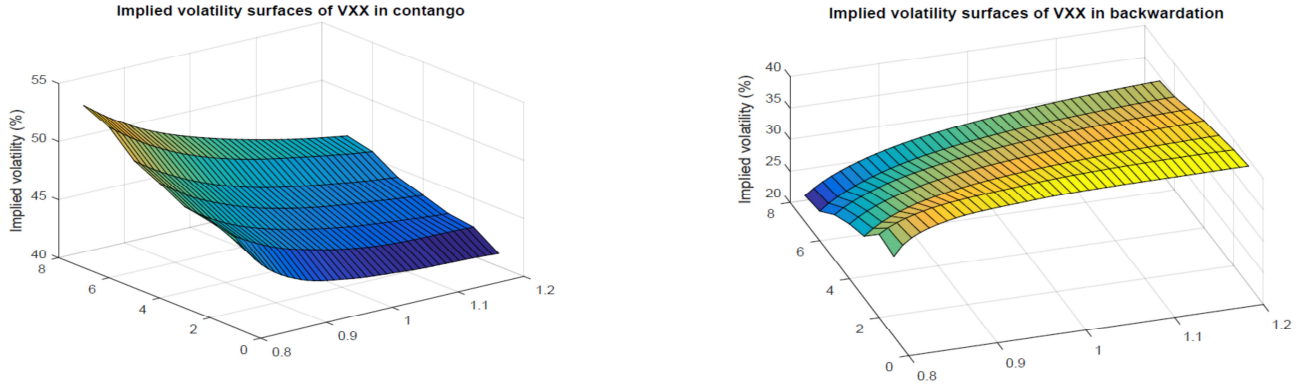


Figure 7: Left: implied volatility surface for the VXX generated when the term structure of futures prices on VIX is in contango with a negative $\delta = -0.1$; Right: implied volatility surface for the VXX generated when the term structure of futures prices on VIX is in backwardation with a positive $\delta = 0.1$. The other parameters are fixed as follows: $X_0 = 0.1, S_0 = 20, VIX_0 = 20, \omega = 1, \kappa = 0.9, \theta = 1.11, \alpha = 0, \beta = 1, \rho = 0.5, r = 0, \sigma = 0.4$. Strikes range between 80% and 120% of the corresponding futures price.

developing consistent modeling and pricing techniques in an environment where products related to the VIX have been flourishing.

9 Appendix

9.1 Some useful transforms

In this section we recall some standard results on the transforms of CIR processes that constitute the building blocks for the computations we have to perform in order to implement our formulae. Here we recall a slight generalisation of the celebrated Pitman and Yor Pitman and Yor (1982) formula giving the joint Laplace transform of the CIR process together with its integral.

Let W be a Brownian motion defined on a filtered probability space $(\Omega, \mathcal{F}, (\mathcal{F}_t)_{t \geq 0}, \mathbb{Q})$.

Lemma 9.1. *Let y be a Cox–Ingersoll–Ross (CIR) process, i.e.*

$$dy_t = \kappa(\theta - y_t)dt + \omega\sqrt{y_t}dW_t \quad (32)$$

with $2\kappa\theta \geq \omega^2$ (Feller condition). If

$$\mu \geq -\frac{\kappa^2}{2\omega^2}, \quad (33)$$

$$\lambda \geq -\frac{\sqrt{A} + \kappa}{\omega^2} \quad (34)$$

then for all $t \geq 0$

$$\mathbb{E} \left[e^{-\mu \int_0^t y_s ds - \lambda y_t} \right] = e^{\phi(0, t, \mu, \lambda) + y_0 \psi(0, t, \mu, \lambda)}, \quad (35)$$

where

$$\phi(0, t, \mu, \lambda) = -\frac{2\theta\kappa}{\omega^2} \ln \left(\frac{(\omega^2\lambda + \kappa)(e^{\sqrt{A}t} - 1) + \sqrt{A}(e^{\sqrt{A}t} + 1)}{2\sqrt{A}e^{\frac{\sqrt{A}+\kappa}{2}t}} \right), \quad (36)$$

$$\psi(0, t, \mu, \lambda) = \frac{(\lambda\kappa - 2\mu)(e^{\sqrt{A}t} - 1) - \lambda\sqrt{A}(e^{\sqrt{A}t} + 1)}{(\omega^2\lambda + \kappa)(e^{\sqrt{A}t} - 1) + \sqrt{A}(e^{\sqrt{A}t} + 1)}, \quad (37)$$

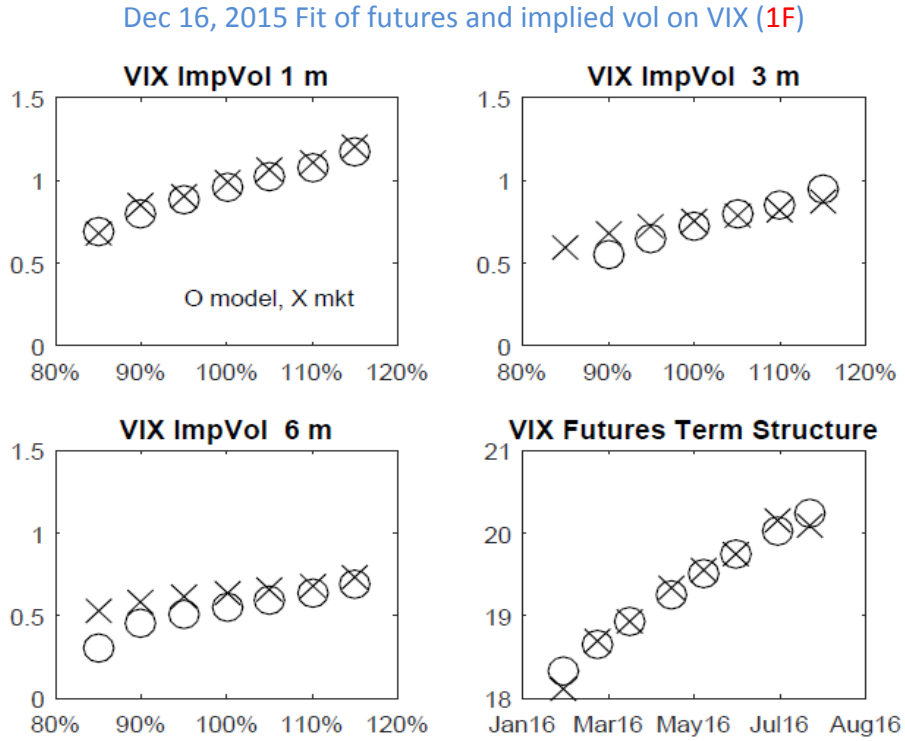


Figure 8: Fit of the term structure of futures prices on VIX and the implied volatility surface on market data as on Dec 16, 2015, where the VIX value was 17,86%. Model prices are in circles, market quotes are crossed. Calibrated parameters in the one-factor specification of the model: $Y_0 = 9.757, \tilde{\omega} = 10.0, \tilde{\kappa} = 11.683, \tilde{\theta} = 0.387, \tilde{\alpha} = 3.133, \tilde{\beta} = 0.413, \tilde{\rho} = 0.931, \tilde{\delta} = -0.0211, \tilde{\sigma} = 0.209, \tilde{\bar{\delta}} = 0.11$. The Resnorm is 5.32^*e-5 .

with $A = \kappa^2 + 2\mu\omega^2$. If

$$\lambda < -\frac{\sqrt{A} + \kappa}{\omega^2}, \quad (38)$$

then the transform (35) is valid up to the maximal time t_{max} given by

$$t_{max} = \frac{1}{\sqrt{A}} \ln \left(1 - \frac{2\sqrt{A}}{\kappa + \omega^2\lambda + \sqrt{A}} \right). \quad (39)$$

The result is standard, for a proof see e.g. Theorem A.1 in Grasselli (2017), where it is shown that the result is valid also for $\mu = -\frac{\kappa^2}{2\omega^2}$ by taking the limit for $A \rightarrow 0$.

Using the Lemma 9.1, we get the following result.

Lemma 9.2. Let X be the process given in (2)

$$dX_t = \kappa(\theta - X_t)dt + \omega\sqrt{\alpha X_t + \beta}dW_t, \quad X_0 = x. \quad (40)$$

i) Let be $\alpha = 0$, then for all $T-t \geq 0$ and for all $\lambda, \mu \in \mathbb{R}$ the joint Laplace transform $\mathbb{E}_t \left[e^{-\mu \int_t^T X_s ds - \lambda X_T} \right]$ is well defined and given by

$$\mathbb{E}_t \left[e^{-\mu \int_t^T X_s ds - \lambda X_T} \right] = e^{\phi(t, T, \mu, \lambda, 0) + X_t \psi(t, T, \mu, \lambda, 0)}, \quad (41)$$

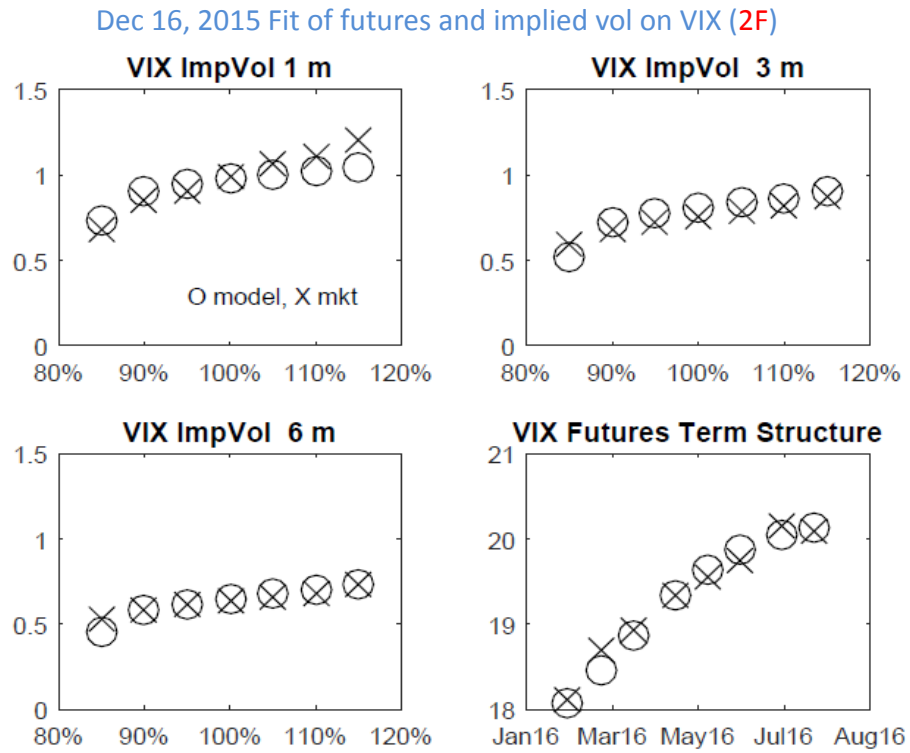


Figure 9: Fit of the term structure of futures prices on VIX and the implied volatility surface on market data as on Dec 16, 2015, where the VIX value was 17.86% in the two factor specification of the model. Model prices are in circles, market quotes are crossed. Calibrated parameters in the two-factor specification of the model: $Y_{10} = 7.454, Y_{20} = 6.143, \tilde{\omega}_1 = 0.070, \tilde{\omega}_2 = 0.816, \tilde{\kappa}_1 = 1.0, \tilde{\kappa}_2 = 10.089, \tilde{\theta}_1 = 8.648, \tilde{\theta}_2 = 7.0, \tilde{\alpha}_1 = 0, \tilde{\alpha}_2 = 1, \tilde{\rho}_1 = -0.86, \tilde{\rho}_2 = -0.988, \tilde{\delta}_1 = 0.928, \tilde{\delta}_2 = -1, \tilde{\sigma}_1 = 1.34, \tilde{\sigma}_2 = 0.5, \bar{\delta} = 0.247$. The Resnorm is 1.14×10^{-5} .

where

$$\psi(t, T, \mu, \lambda, 0) = -\lambda e^{-\kappa(T-t)} - \frac{\mu}{\kappa}(1 - e^{-\kappa(T-t)}), \quad (42)$$

$$\phi(t, T, \mu, \lambda, 0) = \theta \left(\frac{\mu}{\kappa} - \lambda \right) (1 - e^{-\kappa(T-t)}) - \mu \theta (T-t) + \frac{1}{2} \omega^2 \beta \int_t^T \psi(s, T, \mu, \lambda, 0)^2 ds. \quad (43)$$

ii) Let be $\alpha > 0$ and $2\kappa(\alpha\theta + \beta) \geq \omega^2\alpha^2$ (Feller condition). If

$$\mu \geq -\frac{\kappa^2}{2\omega^2\alpha}, \quad (44)$$

$$\lambda \geq -\frac{\sqrt{A} + \kappa}{\omega^2\alpha} \quad (45)$$

then for all $T - t \geq 0$

$$\mathbb{E}_t \left[e^{-\mu \int_t^T X_s ds - \lambda X_T} \right] = e^{\phi(t, T, \mu, \lambda, \alpha) + X_t \psi(t, T, \mu, \lambda, \alpha)}, \quad (46)$$

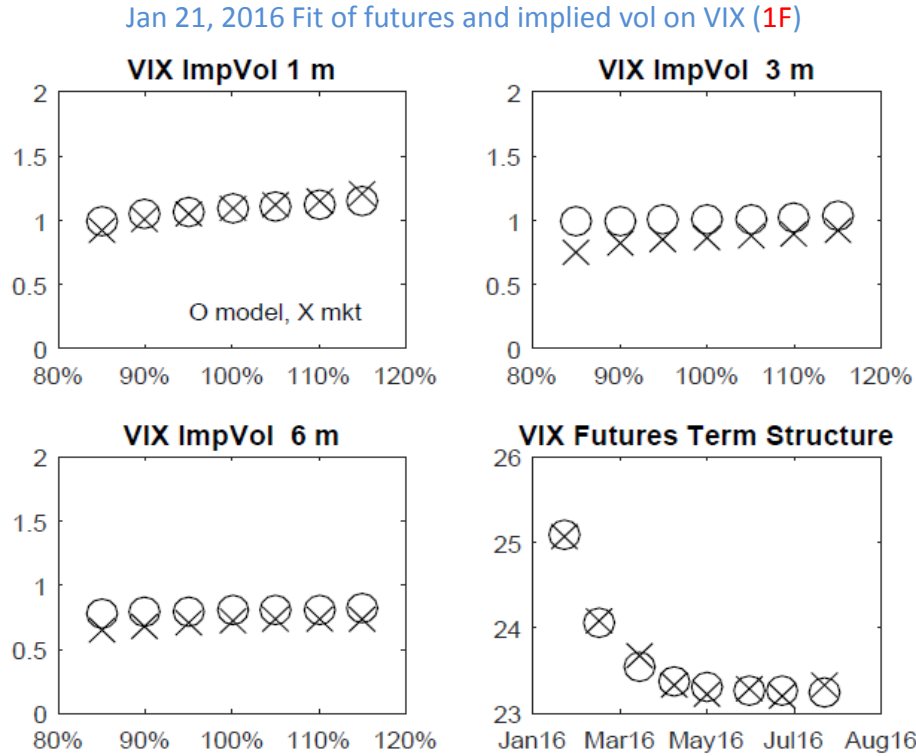


Figure 10: Fit of the term structure of futures prices on VIX and the implied volatility surface on market data as on Jan 21, 2016, where the VIX value was 26,69%. Model prices are in circles, market quotes are crossed. Calibrated parameters in the one-factor specification of the model: $Y_0 = 11.12$, $\tilde{\omega} = 8.386$, $\tilde{\kappa} = 11.561$, $\tilde{\theta} = 1.898$, $\tilde{\alpha} = 1.335$, $\tilde{\beta} = 8.975$, $\tilde{\rho} = 0.719$, $\tilde{\delta} = 0.1922$, $\tilde{\sigma} = 0.289$, $\tilde{\bar{\delta}} = 0.599$. The Resnorm is 4.42^*e-5 .

where

$$\psi(t, T, \mu, \lambda, \alpha) = \frac{(\lambda\kappa - 2\mu)(e^{\sqrt{A}(T-t)} - 1) - \lambda\sqrt{A}(e^{\sqrt{A}(T-t)} + 1)}{(\omega^2\lambda\alpha + \kappa)(e^{\sqrt{A}(T-t)} - 1) + \sqrt{A}(e^{\sqrt{A}(T-t)} + 1)}, \quad (47)$$

$$\phi(t, T, \mu, \lambda, \alpha) = \frac{\beta}{\alpha}(\mu(T-t) + \lambda) + \frac{\beta}{\alpha}\psi(t, T, \mu, \lambda, \alpha) \quad (48)$$

$$- \frac{2(\alpha\theta + \beta)\kappa}{\omega^2\alpha^2} \ln \left(\frac{(\omega^2\alpha\lambda + \kappa)(e^{\sqrt{A}(T-t)} - 1) + \sqrt{A}(e^{\sqrt{A}(T-t)} + 1)}{2\sqrt{A}e^{\frac{\sqrt{A}+\kappa}{2}(T-t)}} \right), \quad (49)$$

$$(50)$$

with $A = \kappa^2 + 2\mu\omega^2\alpha$. If

$$\lambda < -\frac{\sqrt{A} + \kappa}{\omega^2\alpha}, \quad (51)$$

then the transform (46) is valid up to the maximal time to maturity $(T-t)_{max}$ given by

$$(T-t)_{max} = \frac{1}{\sqrt{A}} \ln \left(1 - \frac{2\sqrt{A}}{\kappa + \omega^2\alpha\lambda + \sqrt{A}} \right). \quad (52)$$

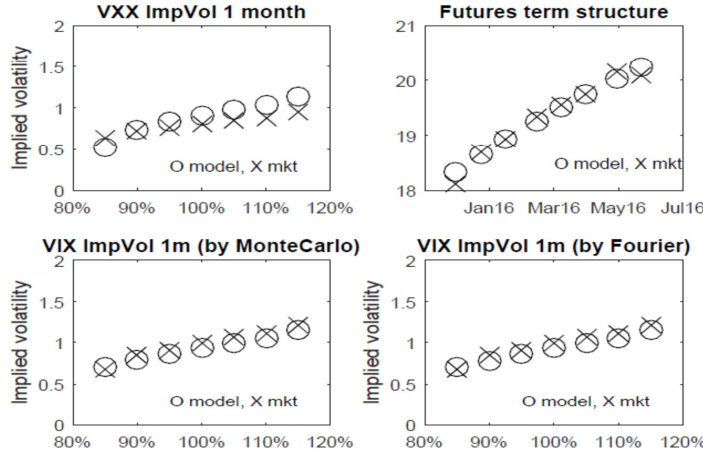


Figure 11: Fit of the VXX implied volatility smile at 1 month with the calibrated model on VIX market data as on Dec 16, 2015, where the VIX value was 17.86% and the VXX was 19.34%. Model prices are in circles, market quotes are crossed. Calibrated parameters in the one-factor specification of the model: $Y_0 = 9.757$, $\tilde{\omega} = 10.0$, $\tilde{\kappa} = 11.683$, $\tilde{\theta} = 0.387$, $\tilde{\alpha} = 3.133$, $\tilde{\beta} = 0.413$, $\tilde{\rho} = 0.931$, $\tilde{\delta} = -0.0211$, $\tilde{\sigma} = 0.209$, $\bar{\delta} = 0.11$. In the bottom of the panel we also display the MonteCarlo prices for the 1 month option on VIX as a double check.

Proof. i) Consider the case $\alpha = 0$, then the process X is Gaussian and standard arguments (see e.g. Subsection 24.3 in Björk (2009)) prove that the functions ϕ, ψ solve the following linear ODE system:

$$\frac{\partial \phi(t, T, \mu, \lambda, 0)}{\partial t} = -\kappa\theta\psi(t, T, \mu, \lambda, 0) - \frac{1}{2}\psi^2(t, T, \mu, \lambda, 0)\omega^2\beta \quad (53)$$

$$\frac{\partial \psi(t, T, \mu, \lambda, 0)}{\partial t} = \kappa\psi(t, T, \mu, \lambda, 0) + \mu, \quad (54)$$

with terminal conditions $\psi(T, T, \mu, \lambda, 0) = -\lambda$ and $\phi(T, T, \mu, \lambda, 0) = 0$. The solution is straightforward and leads to the result.

ii) Consider now $\alpha > 0$, then the process $y_t = \alpha X_t + \beta$ satisfies

$$dy_t = \kappa(\tilde{\theta} - y_t)dt + \omega\alpha\sqrt{y_t}dW_t, \quad (55)$$

with $\tilde{\theta} = \alpha\theta + \beta$. Moreover, in the transform we have to replace $\tilde{\mu} = \frac{\mu}{\alpha}$, $\tilde{\lambda} = \frac{\lambda}{\alpha}$, $\tilde{\omega} = \omega\alpha$. Using Lemma 9.1 we get the result. \square

9.2 Proof of proposition 2.1

The futures price is given by $F(t, T) = \mathbb{E}_t[S_T]$. From (1) it follows immediately that, for $T \geq 0$,

$$S_T = S_0 \exp \left((r - \frac{1}{2}\sigma^2\beta)T - (\delta + \frac{1}{2}\sigma^2\alpha) \int_0^T X_s ds + \sigma \int_0^T \sqrt{\alpha X_s + \beta}(\rho dW_s + \sqrt{1-\rho^2}dW_s^\perp) \right), \quad (56)$$

where W_s^\perp is a Brownian motion independent of W . This implies that:

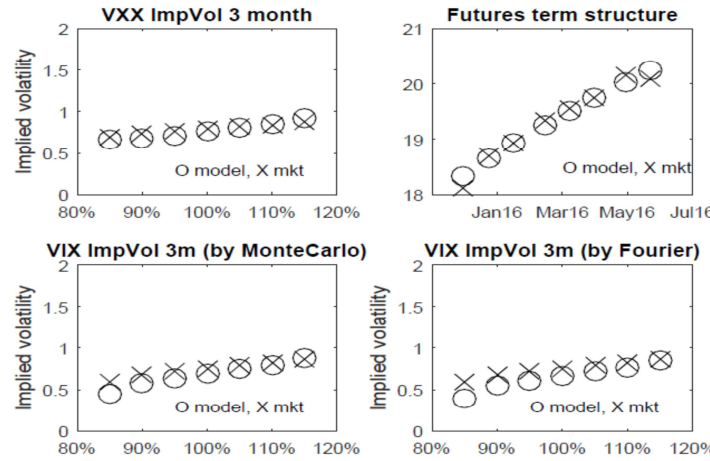


Figure 12: Fit of the VXX implied volatility smile at 3 months with the calibrated model on VIX market data as on Dec 16, 2015, where the VIX value was 17.86% and the VXX was 19.34%. Model prices are in circles, market quotes are crossed. Calibrated parameters in the one-factor specification of the model: $Y_0 = 9.757$, $\tilde{\omega} = 10.0$, $\tilde{\kappa} = 11.683$, $\tilde{\theta} = 0.387$, $\tilde{\alpha} = 3.133$, $\tilde{\beta} = 0.413$, $\tilde{\rho} = 0.931$, $\tilde{\delta} = -0.0211$, $\tilde{\sigma} = 0.209$, $\bar{\delta} = 0.11$. In the bottom of the panel we also display the MonteCarlo prices for the 3 months option on VIX as a double check.

$$F(t, T) = S_t e^{(r - \frac{1}{2}\sigma^2\beta)(T-t)} \quad (57)$$

$$\cdot \mathbb{E}_t [e^{-(\delta + \frac{1}{2}\sigma^2\alpha) \int_t^T X_s ds + \sigma\rho \int_t^T \sqrt{\alpha X_s + \beta} dW_s} \mathbb{E}[e^{\sigma\sqrt{1-\rho^2} \int_t^T \sqrt{\alpha X_s + \beta} dW_s^\perp} | \mathcal{F}_X]] \quad (58)$$

$$= S_t \exp \left((r - \frac{1}{2}\sigma^2\rho^2\beta - \frac{\sigma\rho\kappa\theta}{\omega})(T-t) - \frac{\sigma\rho}{\omega} X_t \right) \quad (59)$$

$$\cdot \mathbb{E}_t \left[\exp \left(-(\delta + \frac{1}{2}\sigma^2\rho^2\alpha - \frac{\sigma\rho\kappa}{\omega}) \int_t^T X_s ds + \frac{\sigma\rho}{\omega} X_T \right) \right] \quad (60)$$

using the fact that W^\perp is independent from \mathcal{F}_X and that

$$\int_t^T \sqrt{\alpha X_s + \beta} dW_s = \frac{1}{\omega} \left(X_T - X_t - \kappa\theta(T-t) + \kappa \int_t^T X_s ds \right) \quad (61)$$

We now apply Lemma 9.2 in the appendix and we get

$$F(t, T) = S_t e^{\Phi(t, T) + X_t \Psi(t, T)}, \quad (62)$$

with

$$\Phi(t, T) = (r - \frac{1}{2}\sigma^2\rho^2\beta - \frac{\sigma\rho\kappa\theta}{\omega})(T-t) + \phi(t, T, \delta + \frac{1}{2}\sigma^2\rho^2\alpha - \frac{\sigma\rho\kappa}{\omega}, -\frac{\sigma\rho}{\omega}, \alpha), \quad (63)$$

$$\Psi(t, T) = \psi(t, T, \delta + \frac{1}{2}\sigma^2\rho^2\alpha - \frac{\sigma\rho\kappa}{\omega}, -\frac{\sigma\rho}{\omega}, \alpha) - \frac{\sigma\rho}{\omega} \quad (64)$$

The functions $\phi(t, T, \mu, \lambda, \alpha), \psi(t, T, \mu, \lambda, \alpha)$ are given in Lemma 9.2 according to the cases $\alpha = 0$ or $\alpha > 0$.

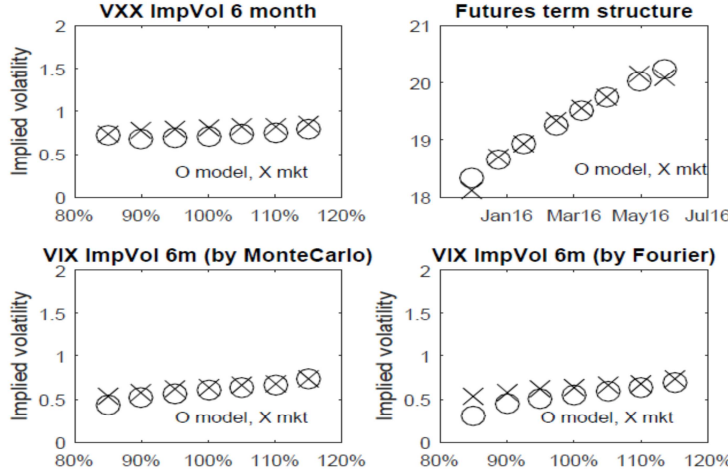


Figure 13: Fit of the VXX implied volatility smile at 6 months with the calibrated model on VIX market data as on Dec 16, 2015, where the VIX value was 17.86% and the VXX was 19.34%. Model prices are in circles, market quotes are crossed. Calibrated parameters in the one-factor specification of the model: $Y_0 = 9.757$, $\tilde{\omega} = 10.0$, $\tilde{\kappa} = 11.683$, $\tilde{\theta} = 0.387$, $\tilde{\alpha} = 3.133$, $\tilde{\beta} = 0.413$, $\tilde{\rho} = 0.931$, $\tilde{\delta} = -0.0211$, $\tilde{\sigma} = 0.209$, $\bar{\delta} = 0.11$. In the bottom of the panel we also display the MonteCarlo prices for the 6 months option on VIX as a double check.

9.3 Proof of proposition 2.2

In order to calculate option prices on VIX, we compute the Fourier transform of the log price $\mathbb{E}[e^{i\epsilon \ln(S_T)}]$. Given (56), (61) and the fact that W^\perp is independent from \mathcal{F}_X , this quantity is equal to:

$$\mathbb{E}[e^{i\epsilon \ln(S_T)}] = e^{i\epsilon \left(\ln(S_0) + (r - \frac{\sigma^2 \beta}{2})T - \frac{\sigma \rho}{\omega} (X_0 + \kappa \theta T) \right) - \frac{\sigma^2 \beta \epsilon^2}{2} (1 - \rho^2) T} \quad (65)$$

$$\times \mathbb{E} \left[e^{\left(-i\epsilon(\delta + \frac{\sigma^2 \alpha}{2} - \frac{\sigma \rho \kappa}{\omega}) - \frac{\sigma^2 \alpha \epsilon^2}{2} (1 - \rho^2) \right) \int_0^T X_s ds + \frac{i\epsilon \sigma \rho}{\omega} X_T} \right] \quad (66)$$

which gives

$$\mathbb{E}[e^{i\epsilon \ln(S_T)}] = e^{i\epsilon \left(\ln(S_0) + (r - \frac{\sigma^2 \beta}{2})T - \frac{\sigma \rho}{\omega} (X_0 + \kappa \theta T) \right) - \frac{\sigma^2 \beta \epsilon^2}{2} (1 - \rho^2) T + \phi(0, T, \mu, \lambda, \alpha) + X_0 \psi(0, T, \mu, \lambda, \alpha)} \quad (67)$$

with

$$\mu = i\epsilon(\delta + \frac{\sigma^2 \alpha}{2} - \frac{\sigma \rho \kappa}{\omega}) + \frac{\sigma^2 \alpha \epsilon^2}{2} (1 - \rho^2) \quad (68)$$

$$\lambda = -\frac{i\epsilon \sigma \rho}{\omega} \quad (69)$$

and ϕ and ψ are given explicitly in Lemma 9.2.

Let us now consider the pricing of a Call on the VIX: standard arguments (see e.g. Carr and Madan (1999)) based on the Fourier techniques show that the price at time $t = 0$ of a Call on the VIX with strike price K and maturity T is given by

$$Call_{VIX}(0) = e^{-rT} \mathbb{E}[(S_T - K)^+] \quad (70)$$

$$= e^{-rT} \int_{\mathbb{R}} (e^{\ln S_T} - K)^+ f(\ln S_T) d \ln S_T, \quad (71)$$

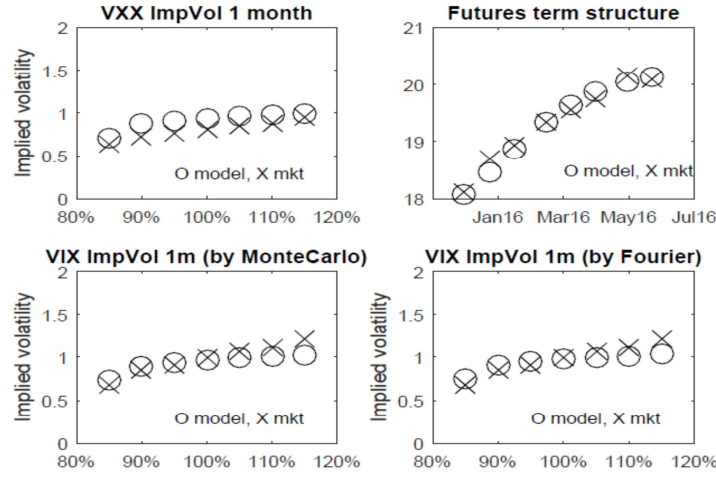


Figure 14: Fit of the VXX implied volatility smile at 1 month with the 2 factor specification of the calibrated model on VIX market data as on Dec 16, 2015, where the VIX value was 17.86% and the VXX was 19.34%. Model prices are in circles, market quotes are crossed. Calibrated parameters in the two-factor specification of the model: $Y_{10} = 7.454, Y_{20} = 6.143, \tilde{\omega}_1 = 0.070, \tilde{\omega}_2 = 0.816, \tilde{\kappa}_1 = 1.0, \tilde{\kappa}_2 = 10.089, \tilde{\theta}_1 = 8.648, \tilde{\theta}_2 = 7.0, \tilde{\alpha}_1 = 0, \tilde{\alpha}_2 = 1, \tilde{\rho}_1 = -0.86, \tilde{\rho}_2 = -0.988, \tilde{\delta}_1 = 0.928, \tilde{\delta}_2 = -1, \tilde{\sigma}_1 = 1.34, \tilde{\sigma}_2 = 0.5, \bar{\delta} = 0.247$. In the bottom of the panel we also display the MonteCarlo prices for the 1 month option on VIX as a double check.

where $f(\ln S_T)$ denotes the risk neutral density of the log price of the VIX. This density can be recovered through the Fourier inversion:

$$f(\ln S_T) = \frac{1}{2\pi} \int_{-\infty}^{+\infty} e^{-i\epsilon \ln S_T} \mathbb{E}[e^{i\epsilon \ln(S_T)}] d\epsilon, \quad (72)$$

so that

$$\text{Call}_{VIX}(0) = e^{-rT} \int_{\mathbb{R}} (e^y - K)^+ \frac{1}{2\pi} \int_{-\infty}^{+\infty} e^{-i\epsilon y} \mathbb{E}[e^{i\epsilon \ln(S_T)}] d\epsilon dy \quad (73)$$

$$= \frac{e^{-rT}}{2\pi} \int_{-\infty}^{+\infty} \mathbb{E}[e^{i\epsilon \ln(S_T)}] \int_{\mathbb{R}} (e^y - K)^+ e^{-i\epsilon y} dy d\epsilon. \quad (74)$$

In the previous equality we implicitly assumed that the condition for the Fubini's theorem hold true. However, as the payoff function is not in L^1 one should extend the notion of Fourier transform to the so-called generalized Fourier (or Laplace-Laplace) transform, which basically takes a complex ϵ in order to grant integrability. We perform the change of variable $\epsilon \rightarrow -\epsilon$ and in the inner integral we can recognize the generalized Fourier transform of the Call payoff, which is given by

$$\int_{\mathbb{R}} (e^y - K)^+ e^{iy} dy = - \frac{K^{1+i\epsilon}}{\epsilon^2 - i\epsilon}, \quad (75)$$

provided that $Im(\epsilon) > 1$, where $Im(z)$ denotes the imaginary part of the complex number z . We get

$$\text{Call}_{VIX}(0) = - \frac{e^{-rT}}{2\pi} \int_{\mathcal{D}} \mathbb{E}[e^{-i\epsilon \ln(S_T)}] \frac{K^{1+i\epsilon}}{\epsilon^2 - i\epsilon} d\epsilon, \quad (76)$$

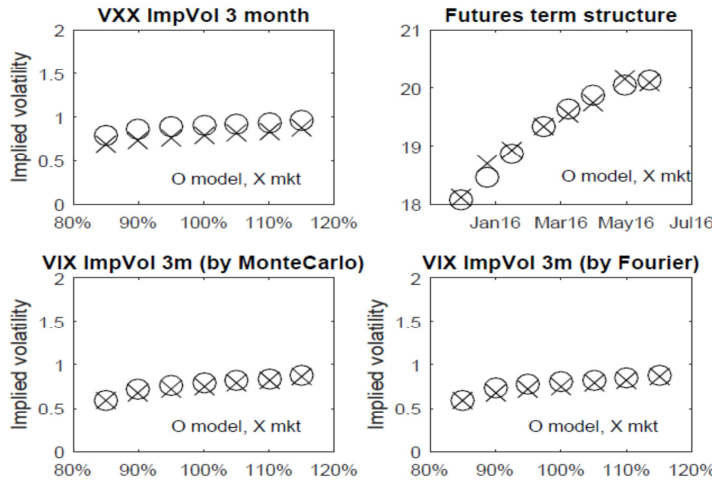


Figure 15: Fit of the VXX implied volatility smile at 3 months with the 2 factor specification of the calibrated model on VIX market data as on Dec 16, 2015, where the VIX value was 17.86% and the VXX was 19.34%. Model prices are in circles, market quotes are crossed. Calibrated parameters in the two-factor specification of the model: $Y_{10} = 7.454, Y_{20} = 6.143, \tilde{\omega}_1 = 0.070, \tilde{\omega}_2 = 0.816, \tilde{\kappa}_1 = 1.0, \tilde{\kappa}_2 = 10.089, \tilde{\theta}_1 = 8.648, \tilde{\theta}_2 = 7.0, \tilde{\alpha}_1 = 0, \tilde{\alpha}_2 = 1, \tilde{\rho}_1 = -0.86, \tilde{\rho}_2 = -0.988, \tilde{\delta}_1 = 0.928, \tilde{\delta}_2 = -1, \tilde{\sigma}_1 = 1.34, \tilde{\sigma}_2 = 0.5, \bar{\delta} = 0.247$. In the bottom of the panel we also display the MonteCarlo prices for the 3 months option on VIX as a double check.

where the integration is on an horizontal line at a level greater than 1, that is $\mathcal{D} = \mathbb{R} \times Im(z)$. Finally, we arrive to

$$Call_{VIX}(0) = -\frac{e^{-rT}K}{\pi} \int_0^{+\infty} Re \left[\frac{K^{i\epsilon}}{\epsilon^2 - i\epsilon} \mathbb{E}[e^{-i\epsilon \ln(S_T)}] \right] d\epsilon, \quad (77)$$

where by symmetry (the function inside was even) the integration is performed with respect to the positive real part of ϵ by fixing the imaginary part to be greater than 1. Typically (see e.g. Carr and Madan (1999)) one takes $\epsilon = p + i\alpha$ with $\alpha = 1.1$.

9.4 n -factor specification

We present here a model where the dynamics of the VIX is driven by n independent factors and that generalizes the one-factor specification framework given by (2) and (1) and that is used throughout the paper. Consider n independent factors $X^{(1)}, \dots, X^{(n)}$ such that:

$$dX_t^{(j)} = \kappa_j(\theta_j - X_t^{(j)})dt + \omega \sqrt{\alpha_j X_t^{(j)} + \beta_j} dW_t^{(j)}, \quad X_0^{(j)} = x^{(j)}, \quad 1 \leq j \leq n \quad (78)$$

Here $W^{(1)}, \dots, W^{(n)}$ are independent Brownian motions. Once again, the coefficient ω is here redundant but is useful when studying developments, which can be calculated following the exact same methodology as in the one-factor model. The dynamics of the VIX is given by:

$$\frac{dS_t}{S_t} = \left[r - \sum_{j=1}^n \delta_j X_t^{(j)} \right] dt + \sum_{j=1}^n \sigma_j \sqrt{\alpha_j X_t^{(j)} + \beta_j} dZ_t^{(j)}, \quad S_0 > 0, \quad (79)$$

where $Z^{(1)}, \dots, Z^{(n)}$ are independent Brownian motions such that:

$$\text{corr}(Z^{(j)}, W^{(j)}) = \rho_j \quad 1 \leq j \leq n$$

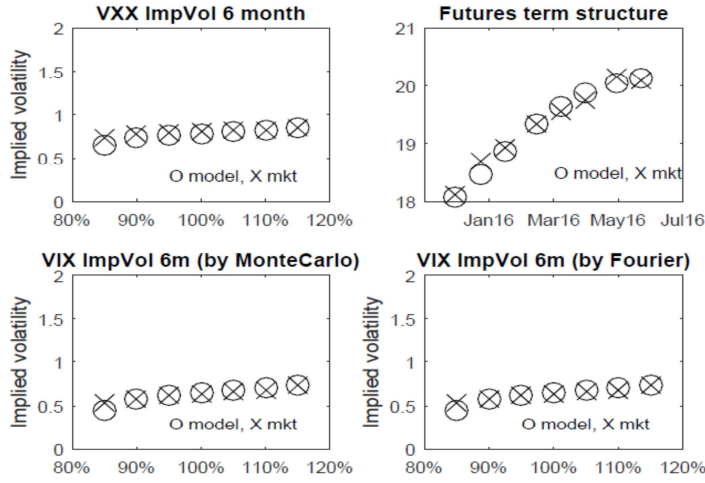


Figure 16: Fit of the VXX implied volatility smile at 6 months with the 2 factor specification of the calibrated model on VIX market data as on Dec 16, 2015, where the VIX value was 17.86% and the VXX was 19.34%. Model prices are in circles, market quotes are crossed. Calibrated parameters in the two-factor specification of the model: $Y_{10} = 7.454, Y_{20} = 6.143, \tilde{\omega}_1 = 0.070, \tilde{\omega}_2 = 0.816, \tilde{\kappa}_1 = 1.0, \tilde{\kappa}_2 = 10.089, \tilde{\theta}_1 = 8.648, \tilde{\theta}_2 = 7.0, \tilde{\alpha}_1 = 0, \tilde{\alpha}_2 = 1, \tilde{\rho}_1 = -0.86, \tilde{\rho}_2 = -0.988, \tilde{\delta}_1 = 0.928, \tilde{\delta}_2 = -1, \tilde{\sigma}_1 = 1.34, \tilde{\sigma}_2 = 0.5, \bar{\delta} = 0.247$. In the bottom of the panel we also display the MonteCarlo prices for the 6 months option on VIX as a double check.

$$\text{corr}(Z^{(j)}, W^{(k)}) = 0 \quad 1 \leq j \neq k \leq n$$

In order to calculate the future prices and (call) option prices for the VIX in the n -factor model, one only needs to calculate the Fourier transform of the log price, that is $\mathbb{E}[e^{i\epsilon \ln(S_T)}]$. Given that $X^{(1)}, \dots, X^{(n)}$ are independent factors and following the calculations of section 2, it follows directly that:

$$\mathbb{E}[e^{i\epsilon \ln(S_T)}] = e^{i\epsilon \left(\ln(S_0) + rT - \sum_{j=1}^n \left[\frac{\sigma_j^2 \beta_j}{2} T + \frac{\sigma_j \rho_j}{\omega} (X_0^{(j)} + \kappa_j \theta_j T) \right] \right)} \quad (80)$$

$$\times e^{\sum_{j=1}^n \left[\frac{-\sigma_j^2 \beta_j \epsilon^2}{2} (1 - \rho_j^2) T + \phi(0, T, \mu_j, \lambda_j, \alpha_j) + X_0^{(j)} \psi(0, T, \mu_j, \lambda_j, \alpha_j) \right]} \quad (81)$$

with

$$\mu_j = i\epsilon(\delta_j + \frac{\sigma_j^2 \alpha_j}{2} - \frac{\sigma_j \rho_j \kappa_j}{\omega}) + \frac{\sigma_j^2 \alpha_j \epsilon^2}{2} (1 - \rho_j^2) \quad (82)$$

$$\lambda_j = -\frac{i\epsilon \sigma_j \rho_j}{\omega} \quad (83)$$

and ϕ and ψ are given explicitly in Lemma 9.2.

9.5 Integral calculations

Let us consider the case of a maturity $T \leq T_1$, so we compute here the terms $\int_0^T \gamma(s) ds$ and $\int_0^T \gamma^2(s) ds$. Recall that for $0 \leq t \leq T_1$:

$$a(t) = \frac{T_1 - t}{T_2 - T_1} = \frac{T_1 - t}{\tau}. \quad (84)$$

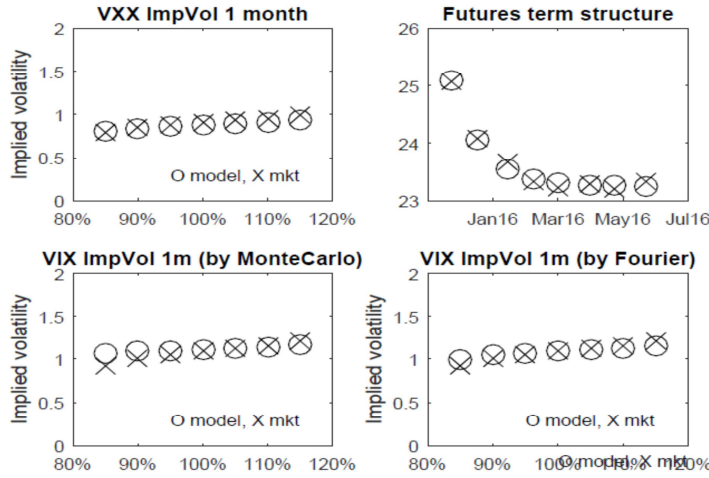


Figure 17: Fit of the VXX implied volatility smile at 1 month with the calibrated model on VIX market data as on Jan 21, 2016, where the VIX value was 26.69% and the VXX was 27.29%. Model prices are in circles, market quotes are crossed. Calibrated parameters in the one-factor specification of the model: $Y_0 = 11.12$, $\tilde{\omega} = 8.386$, $\tilde{\kappa} = 11.561$, $\tilde{\theta} = 1.898$, $\tilde{\alpha} = 1.335$, $\tilde{\beta} = 8.975$, $\tilde{\rho} = 0.719$, $\tilde{\delta} = 0.1922$, $\tilde{\sigma} = 0.289$, $\bar{\delta} = 0.599$. In the bottom of the panel we also display the MonteCarlo prices for the 1 month option on VIX as a double check.

We get

$$\begin{aligned}
 \int_0^T \gamma(s) ds &= \int_0^T \frac{T_1 - s}{\tau} e^{-\kappa(T_1-s)} ds + \int_0^T \left(1 - \frac{T_1 - s}{\tau}\right) e^{-\kappa(T_2-s)} ds \\
 &= \int_0^T \frac{T_1 - s}{\tau} e^{-\kappa(T_1-s)} ds + \int_0^T \frac{s}{\tau} e^{-\kappa(T_2-s)} ds \\
 &= \frac{T_1 e^{-\kappa T_1}}{\tau} \int_0^T e^{\kappa s} ds + \frac{e^{-\kappa T_2} - e^{-\kappa T_1}}{\tau} \int_0^T s e^{\kappa s} ds \\
 &= \frac{T_1 e^{-\kappa T_1}}{\tau} \left(\frac{e^{\kappa T} - 1}{\kappa} \right) + \frac{e^{-\kappa T_2} - e^{-\kappa T_1}}{\tau} \left(\frac{T e^{\kappa T}}{\kappa} - \frac{e^{\kappa T} - 1}{\kappa^2} \right)
 \end{aligned}$$

For the second integral let us introduce the following notation.

$$\begin{aligned}
 c_0 &= \int_0^T e^{2\kappa s} ds = \frac{1}{2\kappa} (e^{2\kappa T} - 1); \\
 c_1 &= \int_0^T s e^{2\kappa s} ds = \frac{T e^{2\kappa T}}{2\kappa} - \frac{1}{4\kappa^2} (e^{2\kappa T} - 1); \\
 c_2 &= \int_0^T s^2 e^{2\kappa s} ds = \frac{T^2 e^{2\kappa T}}{2\kappa} - \frac{T e^{2\kappa T}}{2\kappa^2} + \frac{1}{4\kappa^3} (e^{2\kappa T} - 1);
 \end{aligned}$$

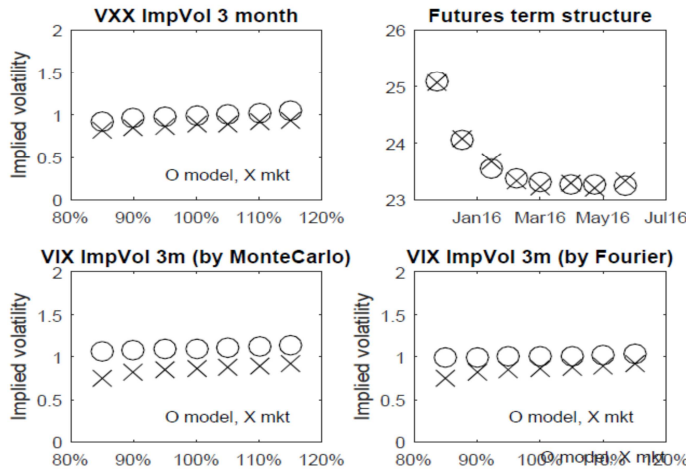


Figure 18: Fit of the VXX implied volatility smile at 3 months with the calibrated model on VIX market data as on Jan 21, 2016, where the VIX value was 26,69% and the VXX was 27,29%. Model prices are in circles, market quotes are crossed. Calibrated parameters in the one-factor specification of the model: $Y_0 = 11.12$, $\tilde{\omega} = 8.386$, $\tilde{\kappa} = 11.561$, $\tilde{\theta} = 1.898$, $\tilde{\alpha} = 1.335$, $\tilde{\beta} = 8.975$, $\tilde{\rho} = 0.719$, $\tilde{\delta} = 0.1922$, $\tilde{\sigma} = 0.289$, $\bar{\delta} = 0.599$. In the bottom of the panel we also display the MonteCarlo prices for the 3 months option on VIX as a double check.

We get

$$\begin{aligned} \int_0^T \gamma^2(s) ds &= \int_0^T \left(\frac{T_1 - s}{\tau} \right)^2 e^{-2\kappa(T_1-s)} ds + \int_0^T \left(1 - \frac{T_1 - s}{\tau} \right)^2 e^{-2\kappa(T_2-s)} ds \\ &\quad + 2 \int_0^T \frac{T_1 - s}{\tau} \left(1 - \frac{T_1 - s}{\tau} \right) e^{-\kappa(T_1+T_2-2s)} ds \\ &= \frac{1}{\tau^2} \left[c_0 \left(T_1^2 e^{-2\kappa T_1} + (\tau - T_1)^2 e^{-2\kappa T_2} + 2T_1(\tau - T_1)e^{-\kappa(T_1+T_2)} \right) \right. \\ &\quad \left. + c_1 \left(-2T_1 e^{-2\kappa T_1} + 2(\tau - T_1)e^{-2\kappa T_2} + 2(2T_1 - \tau)e^{-\kappa(T_1+T_2)} \right) \right. \\ &\quad \left. + c_2 \left(e^{-2\kappa T_1} + e^{-2\kappa T_2} - 2e^{-\kappa(T_1+T_2)} \right) \right] \end{aligned}$$

References

- Alexander, C. and Korovilas, D. (2013). Volatility exchange-traded notes: curse or cure? *The Journal of Alternative Investments*, 16(2):52.
- Avellaneda, M. and Papanicolaou, A. (2017). Statistics of VIX Futures and Applications to Trading Volatility Exchange-Traded Products. *Working Paper*, available at https://papers.ssrn.com/sol3/papers.cfm?abstract_id=3028910.
- Bao, Q., Li, S., and Gong, D. (2012). Pricing vxx option with default risk and positive volatility skew. *European Journal of Operational Research*, 223(1):246–255.
- Barclays (2016). VXX prospectus. available at <http://www.ipathetn.com/US/16/en/contentStore.app?id=5598742>.

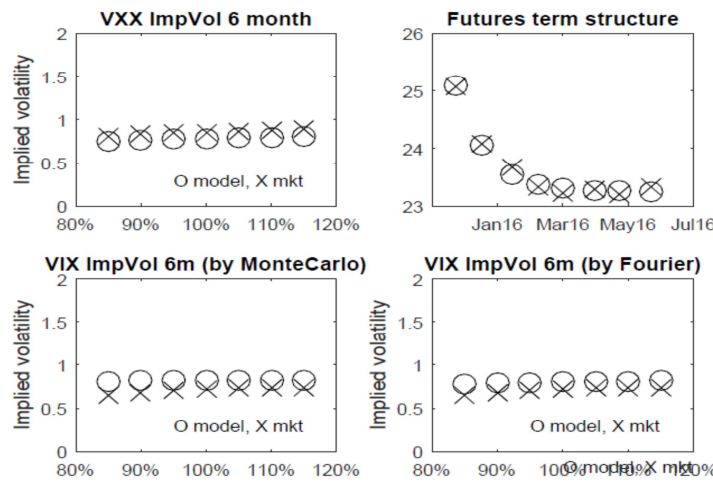


Figure 19: Fit of the VXX implied volatility smile at 6 months with the calibrated model on VIX market data as on Jan 21, 2016, where the VIX value was 26,69% and the VXX was 27,29%. Model prices are in circles, market quotes are crossed. Calibrated parameters in the one-factor specification of the model: $Y_0 = 11.12$, $\tilde{\omega} = 8.386$, $\tilde{\kappa} = 11.561$, $\tilde{\theta} = 1.898$, $\tilde{\alpha} = 1.335$, $\tilde{\beta} = 8.975$, $\tilde{\rho} = 0.719$, $\tilde{\delta} = 0.1922$, $\tilde{\sigma} = 0.289$, $\bar{\delta} = 0.599$. In the bottom of the panel we also display the MonteCarlo prices for the 6 months option on VIX as a double check.

- Bergomi, L. (2016). *Stochastic Volatility Modeling*. Taylor and Francis Group, Boca Raton.
- Björk, T. (2009). *Arbitrage theory in continuous time*. Oxford university press, New York, Third Edition, Oxford.
- Bloomberg (2012). Sec said to review credit suisse vix note. available at <http://www.bloomberg.com/news/articles/2012-03-29/sec-said-to-review-credit-suisse-vix-note>.
- Carmona, R. and Ludkovski, M. (2004). Spot convenience yield models for the energy markets. *Contemporary Mathematics*, 351:65–80.
- Carr, P. and Madan, D. B. (1999). Option valuation using the fast fourier transform. *Journal of Computational Finance*, 2:61–73.
- Cont, R. and Kokholm, T. (2013). A consistent pricing model for index options and volatility derivatives. *Mathematical Finance*, 23(2):248–274.
- Detemple, J. and Osakwe, C. (2000). The valuation of volatility options. *European Finance Review*, 4(1):21–50.
- Galai, D. (1979). A proposal for indexes for traded call options. *The Journal of Finance*, 34(5):1157–1172.
- Gibson, R. and Schwartz, E. S. (1990). Stochastic convenience yield and the pricing of oil contingent claims. *The Journal of Finance*, 45(3):959–976.
- Gourieroux, C. (2006). Continuous time wishart process for stochastic risk. *Econometric Reviews*, 25:177–217.
- Grasselli, M. (2017). The 4/2 Stochastic Volatility Model: a Unified Approach for the Heston and the 3/2 Model. *Mathematical Finance*, 27:1013–1034.

- Grasselli, M. and Tebaldi, C. (2008). Solvable affine term structure models. *Mathematical Finance*, 18(1):135–153.
- Grünbichler, A. and Longstaff, F. A. (1996). Valuing futures and options on volatility. *Journal of Banking & Finance*, 20(6):985–1001.
- Heston, S. L. (1993). A closed-form solution for options with stochastic volatility with applications to bond and currency options. *Review of Financial Studies*, 6:327–343.
- Kaeck, A. and Alexander, C. (2010). VIX dynamics with stochastic volatility of volatility. *ICMA Centre, Henley Business School, University of Reading, UK*.
- Kaeck, A. and Alexander, C. (2013). Continuous-time VIX dynamics: On the role of stochastic volatility of volatility. *International Review of Financial Analysis*, 28:46–56.
- Lin, Y.-N. (2013). Vix option pricing and.cboe vix term structure: A new methodology for volatility derivatives valuation. *Journal of Banking & Finance*, 37(11):4432–4446.
- Mencia, J. and Sentana, E. (2013). Valuation of vix derivatives. *Journal of Financial Economics*, 108(2):367–391.
- Pagan, A. R. and Schwert, G. W. (1990). Alternative models for conditional stock volatility. *Journal of Econometrics*, 45(1):267–290.
- Pitman, J. and Yor, M. (1982). A decomposition of bessel bridges. *Probability Theory and Related Fields*, 59:425–457.
- Psychoyios, D., Dotsis, G., and Markellos, R. (2009). A jump diffusion model for VIX volatility options and futures. *Review of Quantitative Finance and Accounting*, 35(3):245–269.
- Schwert, G. W. (1990). Stock returns and real activity: A century of evidence. *The Journal of Finance*, 45(4):1237–1257.
- Schwert, G. W. (2011). Stock volatility during the recent financial crisis. *European Financial Management*, 17(5):789–805.
- Sussman, A. and Morgan, C. (2012). Risk measurement on demand: Complexity, volatility and regulatory uncertainty. *TABB Group Research*.
- CBOE (2014). The CBOE volatility index - VIX. *White paper available at <https://www.cboe.com/micro/vix/vixwhite.pdf>*.
- CBOE (2016). CBOE holdings reports trading volume for 2015. *White paper available at <http://ir.cboe.com/~media/Files/C/CBOE-IR-V2/press-release/2016/cboe-holdings-volume-report-december-2015.pdf>*.
- Whaley, R. E. (1993). Derivatives on market volatility: Hedging tools long overdue. *The journal of Derivatives*, 1(1):71–84.
- Whaley, R. E. (2008). Understanding VIX. *available at SSRN 1296743*.